NASA/TM–2017-219374

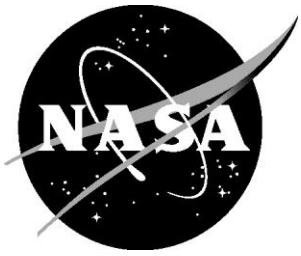

Finite Element Modeling and Analysis of Mars Entry Aeroshell Baseline Concept

Samee W. Ahmed, Brittney M. Lane
Langley Research Center, Hampton, Virginia

June 2017

NASA STI Program . . . in Profile

Since its founding, NASA has been dedicated to the advancement of aeronautics and space science. The NASA scientific and technical information (STI) program plays a key part in helping NASA maintain this important role.

The NASA STI program operates under the auspices of the Agency Chief Information Officer. It collects, organizes, provides for archiving, and disseminates NASA's STI. The NASA STI program provides access to the NTRS Registered and its public interface, the NASA Technical Reports Server, thus providing one of the largest collections of aeronautical and space science STI in the world. Results are published in both non-NASA channels and by NASA in the NASA STI Report Series, which includes the following report types:

- TECHNICAL PUBLICATION. Reports of completed research or a major significant phase of research that present the results of NASA Programs and include extensive data or theoretical analysis. Includes compilations of significant scientific and technical data and information deemed to be of continuing reference value. NASA counter-part of peer-reviewed formal professional papers but has less stringent limitations on manuscript length and extent of graphic presentations.

- TECHNICAL MEMORANDUM. Scientific and technical findings that are preliminary or of specialized interest, e.g., quick release reports, working papers, and bibliographies that contain minimal annotation. Does not contain extensive analysis.

- CONTRACTOR REPORT. Scientific and technical findings by NASA-sponsored contractors and grantees.

- CONFERENCE PUBLICATION. Collected papers from scientific and technical conferences, symposia, seminars, or other meetings sponsored or co-sponsored by NASA.

- SPECIAL PUBLICATION. Scientific, technical, or historical information from NASA programs, projects, and missions, often concerned with subjects having substantial public interest.

- TECHNICAL TRANSLATION. English-language translations of foreign scientific and technical material pertinent to NASA's mission.

Specialized services also include organizing and publishing research results, distributing specialized research announcements and feeds, providing information desk and personal search support, and enabling data exchange services.

For more information about the NASA STI program, see the following:

- Access the NASA STI program home page at http://www.sti.nasa.gov

- E-mail your question to help@sti.nasa.gov

- Phone the NASA STI Information Desk at 757-864-9658

- Write to:
  NASA STI Information Desk
  Mail Stop 148
  NASA Langley Research Center
  Hampton, VA 23681-2199

NASA/TM–2017-219374

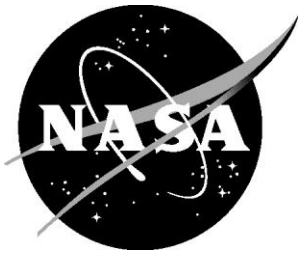

Finite Element Modeling and Analysis of Mars Entry Aeroshell Concept

Samee W. Ahmed, Brittney M. Lane
Langley Research Center, Hampton, Virginia

National Aeronautics and

Space Administration

Langley Research Center

Hampton, Virginia 23681-2199

June 2017

Acknowledgements

This work was made possible by the NASA Internships, Fellowships, Scholarships (NIFS) program at NASA Langley Research Center.

This work was also made possible by Jamshid Samareh and Sandra Walker who supervised and provided us with all of the information and guidance necessary to accomplish our tasks.

In addition, we would further like to acknowledge Sasan Armand and Lance Proctor for providing valuable advice and assistance for our work involving the finite element models.

Finally, we would like to thank the rest of the Vehicle Analysis Branch for helping us in any way they could to complete our work.

Table of Contents

Abstract

The structure that is developed and analyzed in this project must be able to survive all the various load conditions that it will encounter along its course to Mars with the minimal amount of weight and material. At this stage, the goal is to study the capability of the structure using a finite element model (FEM). This FEM is created using a python script, and is numerically solved in Nastran. The purpose of the model is to achieve an optimization of mass given specific constraints on launch and entry. The generation and analysis of the baseline Rigid Mid-Range Lift to Drag Ratio Aeroshell model is a continuation and an improvement on previous work done for the FEM. The model is generated using Python programming with the axisymmetric placement of nodes for beam and shell elements. The shells are assigned a honeycomb sandwich material with an aluminum honeycomb core and composite face sheets, and the beams are assigned the same material as the shell face sheets. There are two load cases assigned to the model: Earth launch and Mars entry. The Earth launch case consists of pressure, gravity, and vibration loads, and the Mars entry case consists of just pressure and gravity loads. The Earth launch case was determined to be the driving case, though the analyses are performed for both cases to ensure the constraints are satisfied. The types of analysis performed with the model are design optimization, statics, buckling, normal modes, and frequency response, the last of which is only for the Earth launch load case. The final results indicated that all of the requirements are satisfied except the thermal limits, which could not yet be tested, and the normal modes for the Mars entry. However, the frequency limits during Mars entry are expected to be much higher than the lower frequency limits set for the analysis. In addition, there are still improvements that can be made in order to reduce the weight while still meeting all requirements.

1 Background

1.1 Description of overall Mid L/D project

The Mid L/D project is focused on the development of Entry, Decent, and Landing (EDL) technology that will be used for delivering large payloads of crew and cargo to the surface of Mars. The structure must be able to withstand the process of launching from Earth and enduring the extreme loads involved when entering the atmosphere of Mars. In addition to the basic pressure loads that originate from aerodynamic effects, the structure must also withstand vibration effects during launch, and extreme heat caused by friction from traveling through the Mars atmosphere at hypersonic speeds. While several different structures had been analyzed to ascertain their feasibility, the design that is primarily considered and is the focus of this report is the Rigid Mid-Range Lift to Drag Ratio Aeroshell (Rigid Mid-L/D AS). Figure 1 shows a diagram of all the structures where Architecture 1 is the focus of this project.

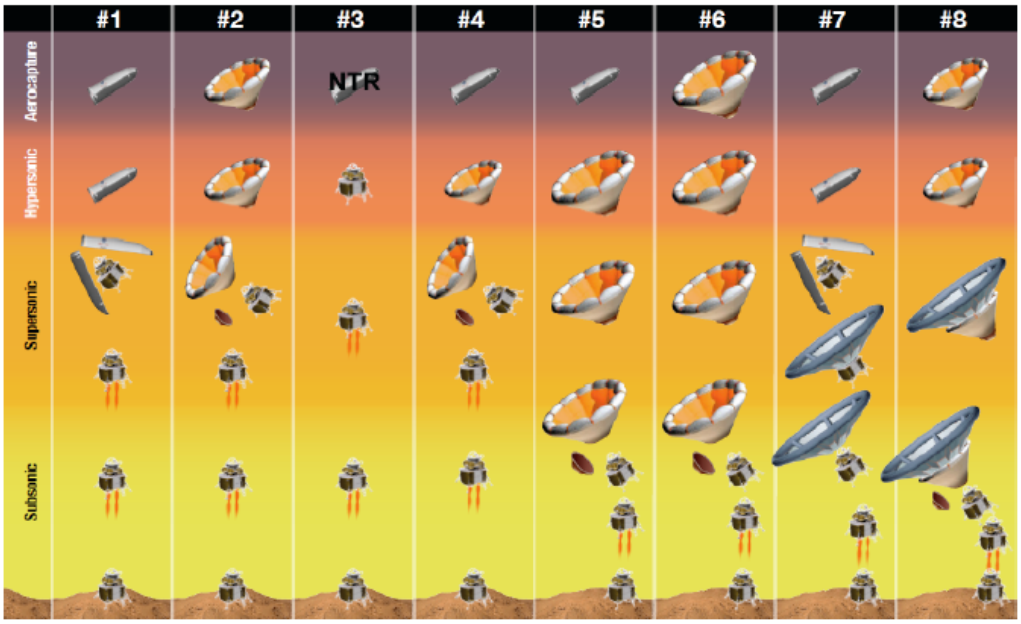

Table 1. Simplified Set of Exploration Class Technologies Considered by EDL-SA

	Aerocapture	Hypersonic	Supersonic	Subsonic
Architecture 1	Rigid Mid-L/D AS	Rigid Mid-L/D AS	Propulsion	Propulsion
Architecture 2	Lifting HIAD	Lifting HIAD	Propulsion	Propulsion
Architecture 3	N/A	Propulsion	Propulsion	Propulsion
Architecture 4	Rigid Mid-L/D AS	Lifting HIAD	Propulsion	Propulsion
Architecture 5	Rigid Mid-L/D AS	Lifting HIAD	Same LHIAD	Propulsion
Architecture 6	Lifting HIAD	Lifting HIAD	Same LHIAD	Propulsion
Architecture 7	Rigid Mid-L/D AS	Rigid Mid-L/D AS	Drag SIAD	Propulsion
Architecture 8	Lifting HIAD	Lifting HIAD	LSIAD–Skirt	Propulsion

Figure 1. Mars Entry Structures

Studies and analyses done previously on all these concepts resulted in Architecture 1 and 2 as the only ones that are still being considered due to having less complexity in their process of EDL. The other structure types have been abandoned either due to impracticality or design issues that were not or could not be solved (Dwyer 2010).

1.1.1 Shape and Structure of the Model

The idealized geometry of the Rigid Mid-L/D model is shown in Figure 2. It is a simple FEM with a stiffened cylindrical body and hemispherical dome. This model is created using python programming.

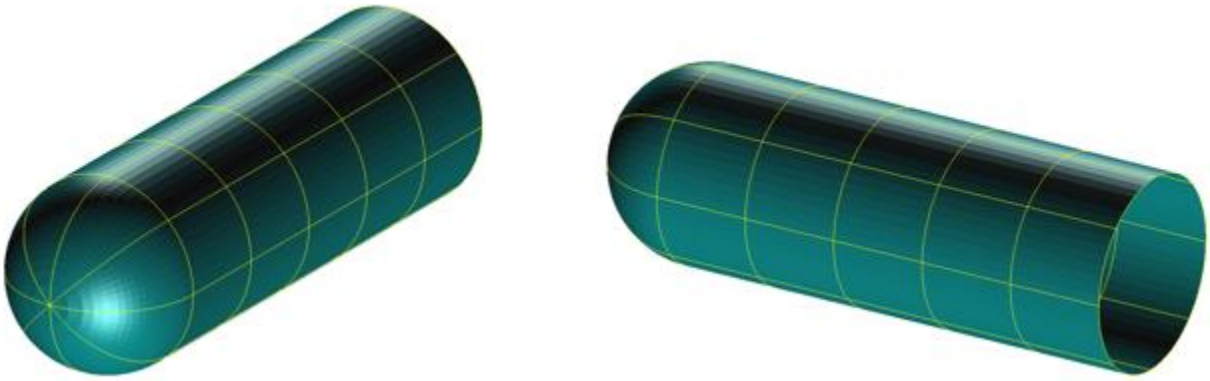

Figure 2. Finite Element Model

The main part of the structure is a relatively thin outer shell layer which houses the payload. This overall shell structure consists of several sections along the length of the structure. The initial concept has its shell layer divided into six sections where the hemisphere at the top end is the first shell section and the cylinder is equally divided into the five other sections. In addition to the shell layer, the inside of the Rigid Mid-L/D model consists of frames and longerons composed of beam elements. The frames are circumferential stiffeners and are located in the cylinder structure at the divisions of the six shell sections, and the longerons are stiffeners that span the entire length of the structure (Dwyer 2010). Figure 3 shows the different sections as well as the placement of the frames and longerons.

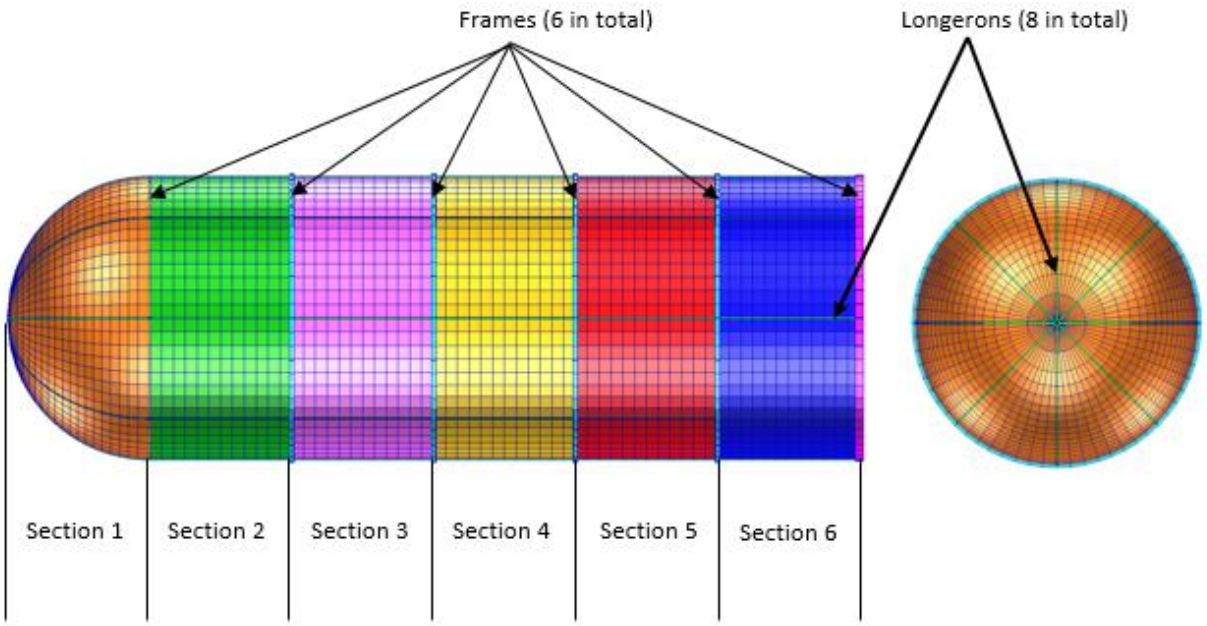

Figure 3. Shell Sections and Stiffeners

While the original structure has the specific attributes shown in the figures above, the new and altered models that have been generated for this study using Python programming can vary in terms of the number of sections, frames, and longerons in order to find an optimized aeroshell for the journey to Mars (Lane 2017). However, the general structure and shape will still remain the same and the placement of the beams will still have the same orientation on the shell structure. In addition, there is one model that will have a specific set of parameter values that will be considered the baseline of the project, and that baseline is the focus of this report. Table 1 shows the different parameter values for the baseline model.

Table 1. Model Parameters and Baseline Values

Dimensions	Diameter (m)	10.0
	Length (m)	30.0
Meshing	Number of Elements Along Cylindrical Edge	60
	Number of elements along circumference	64
Structure	Number Of Frame Rings	6
	Number of Longerons	8
	Number of Shell Sections	6
Mass	Payload Mass (kg)	100,000
TPS	Area Density (kg/m^2)	9.8
Shell Material 1 (core)	Density (kg/m^3)	49.57
	Young's Modulus, E (Pa)	5.17E+08
	Shear Modulus, G (Pa)	1.52E+08
	Thickness: Lower Limit (mm)	10.0
	Thickness: Upper Limit (mm)	1000.0
	Allowable Stress (Pa)	1.48E+06
Shell Material 2 (composite)	Density (kg/m^3)	1580
	Young's Modulus, E (Pa)	5.80E+10
	Shear Modulus, G (Pa)	2.21E+10
	Thickness: Lower Limit (mm)	1.0
	Thickness: Upper Limit (mm)	20.0
	Allowable Stress (Pa)	5.12E+08
Longeron Bar Material	Density (kg/m^3)	1580
	Young's Modulus, E (Pa)	5.80E+10
	Shear Modulus, G (Pa)	2.21E+10
	Thickness: Lower Limit (mm)	5.0
	Thickness: Upper Limit (mm)	300.0
	Allowable Stress (Pa)	5.12E+08
Frame Bar Material	Density (kg/m^3)	1580
	Young's Modulus, E (Pa)	5.80E+10
	Shear Modulus, G (Pa)	2.21E+10
	Thickness: Lower Limit (mm)	5.0
	Thickness: Upper Limit (mm)	300.0
	Allowable Stress (Pa)	5.12E+08
Pressure Loads	Entry: Dynamic Pressure, q (Pa)	5000
	Entry: Angle of Attack, Alpha (Degrees)	55.0
	Entry: Angle of Sideslip, Beta (Degrees)	0.0
	Launch: Dynamic Pressure, q (Pa)	28,100
	Launch: Angle of Attack, Alpha (Degrees)	5.0
	Launch: Angle of Sideslip, Beta (Degrees)	0.0
Launch Vehicle	Lateral	0.75
	Axial	4.00
Entry G Loads	Axial g's	-0.20
	Axial g's Factor of Safety	1.00
	Lateral g's	4.50
	Lateral g's Factor of Safety	1.00

For this project, there are certain materials that are intended to be tested in the future, but due to the lack of test data for these materials they will not be considered in this project. As a result, the material that is used for this project in the test analyses is a composite sandwich made of a honeycomb core and carbon fiber face sheets on both sides of the honeycomb, as well as an ablator to resist major heat transfer during Mars entry. While this composite material can produce useful results for the analyses in this project, the other materials to be studied can possibly prove to be more significant in reducing the weight yet maintaining the capabilities of the structure. An example is a ceramic matrix composite material which acts as both the primary load carrying structure as well as the protection against the extreme heating during Mars entry (Walker 2014). If successful, this could significantly help in reducing the weight as well as the volume of the structure which is an important consideration for launch. The basic idea is to have a composite material on the outside section which is mainly responsible for dealing with the load followed by an insulation blanket on the inside to help regulate the inner temperature. The outer layer composite is intended to be made of an advance carbon-carbon material, though even more capable composite materials may be considered in the future (Walker 2014).

1.1.2 Purpose of the Model

A concise explanation of the goals of this project is that the structure being developed and analyzed has to be able to survive all the various load conditions that it will encounter along its course to Mars with the minimal amount of weight and material that it needs in order to survive without failure. While complete failure must obviously be avoided, the design should also avoid issues dealing with permanent damage such as plastic deformation. Maintaining the original shape and structure is important in order to make sure that the risks of failure are minimized and that it does not lose or reduce the capabilities of the Rigid Mid-L/D.

Out of the different environments that the aeroshell will endure, the two that are significant for the finite element analysis are the launch from Earth and the entry into the Mars atmosphere. For Earth launch, the structure will be under stress from the vibrations during the initial phases of liftoff. Later into the launch, it will experience aerodynamic loads due to reaching high speeds and large gravity loads due to high acceleration. For Mars entry, there will most likely be no significant vibration loads but there will be significant aerodynamic loads as a results of traveling through the Mars atmosphere at hypersonic speeds. The extreme heat associated with this phase will also be another significant load condition that will need to be taken into account.

1.2 Purpose and benefits of analysis

The structural analysis under properly set up loads and boundary conditions can give important insight into the structure and its behavior. Thus, the purpose of the analysis is to determine the different kinds of responses from the structure under certain loads and boundary conditions. The analysis is also used to help determine how variations in the structure design and parameters values will impact the results, which can improve the baseline design. This can be accomplished by using finite element analysis software to identify optimal parameter values. In addition to the design optimization, an automation process has been developed using the Python programming language in order to run a large number of analyses that vary in the parameter values (Lane 2017). The automated design process is used to identify patterns in the vehicle mass reduction and refine the structural design.

The benefits from these different analyses are indispensable and can help identify issues and outcomes of the structural design. The initial benefit of these analyses is that they will provide a virtual layout of the physical aeroshell which satisfies the design requirements. Having a virtual image of the shape and structure of the aeroshell makes it easier and cheaper to understand how the loads and boundary conditions are applied and how the design reacts to them. In addition to visualization, the analyses provide an inexpensive way to determine how the design will react to the given load and boundary conditions. This helps determine weaknesses in the baseline design and potential improvements which satisfy the requirements.

2 Finite Element Model

The finite element model is created by specifying nodes and elements without associated geometry. For this project, the simple shape of the structure allows the finite element mesh to be created without the assistance of geometric entities. The model generation for the structure allows the variation of input parameters, which include the number of nodes and elements in the finite mesh. While more nodes and elements can increase the accuracy of the results, the analysis time will increase. In this stage of developing the Rigid Mid L/D Aeroshell, the number of nodes and elements are limited to reduce the analysis time and still obtain reasonably accurate results to verify the feasibility of the model. To provide the breakdown of the model, Figure 4 shows the model tree that indicates the different parts of the model including the materials, element properties, loads, and load cases. These parts will be described in detail in the sections that follow.

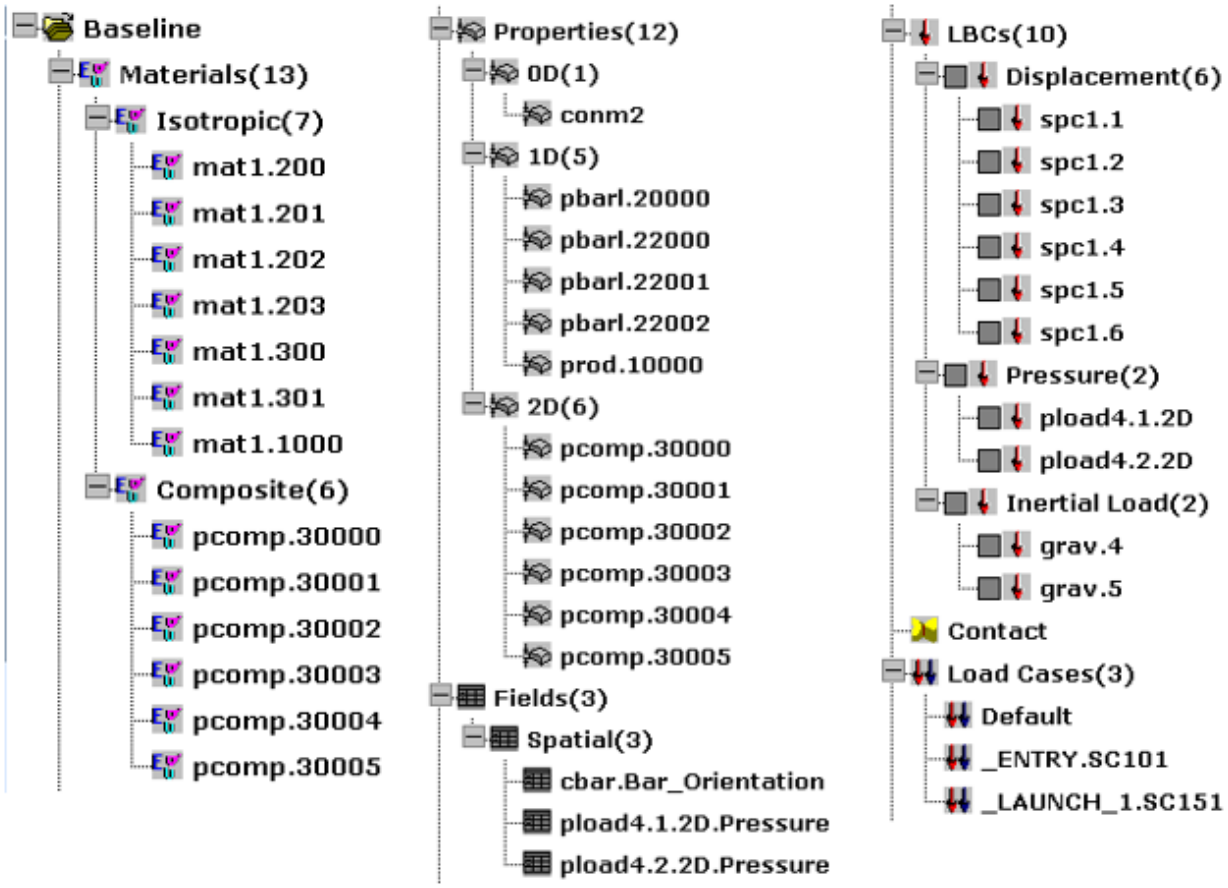

Figure 4. Model Tree from Patran for Baseline Design

2.1 Materials

2.1.1 Composite Sandwich

The material used in the baseline model is a composite sandwich which is made up of a honeycomb core and carbon fiber face sheets. The honeycomb is specifically Hexcel 5052 Alloy Hexagonal Aluminum Honeycomb with a cell size of 0.125 inches (3.175 mm) and a surface thickness of 0.0007 inches (0.01778 mm). Figure 5 below shows the dimensions that represent the cell size and the surface thickness for each hexagon cell in the honeycomb core, and Table 2 shows the material property values for the honeycomb core (HyperSizer, 1998).

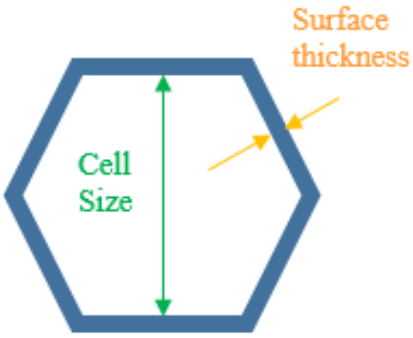

Figure 5. Honeycomb Dimensions

Table 2. Honeycomb Core Material Properties

CORE MATERIAL	
5052 Alloy Hexagonal Aluminum Honeycomb	
Density (kg/m^3)	49.547
Elastic Modulus [E]	MPa
Tension	517.12
Compression	517.12
Shear Modulus [G]	MPa
Transverse	151.68
Longitudinal	310.26
Tension and Shear Ultimate Stress	kPa
Tension	1482.37
Shear (Transverse)	620.53
Shear (Longitudinal)	1068.69
Compression Ultimate Stress	kPa
Stabilized	1482.37
Bare	1378.95
Crush	896.32

The two face sheets labeled as IM7/977-3 [0/+-45/90] are made from HexTow IM7 Carbon Fiber and CYTECH CYCOM 977-3 epoxy resin. Each laminate consists of ply layers that are laid such that the first ply is at 0 degrees to a reference axis, the second is at 45 degrees, the third is at -45 degrees, and the fourth is at 90 degrees. Table 3 shows the material properties of each ply layer and the material properties of each layer of laminate, also known as the effective material properties (HyperSizer, 1998). Note that given the fact that the model uses a composite material rather than some kind of isotropic material, the main stress values that are reported are major principal stresses instead of von Mises stresses.

Table 3. Face Sheet Material Properties

FACESHEET MATERIAL		
HexTow IM7 Carbon Fiber CYCOM 977-3 epoxy resin	Single ply layer	Effective laminate layer
Density (kg/m^3)	1577.76	1577.76
Poisson ratio	unitless	unitless
Tension	0.329	0.313
Compression	0.329	0.313
Elastic Modulus [E]	GPa	GPa
Tension, 0 degrees	152.93	57.95
Tension, 90 degrees	8.89	57.95
Compression, 0 degrees	149.82	56.92
Compression, 90 degrees	8.89	56.92
Shear Modulus [G]	GPa	GPa
In-plane 12	4895.28	22.067
Interlaminar 13	4895.28	no data
Interlaminar 23	2909.59	no data
Tension Ultimate Stress	MPa	MPa
In-plane, 0 degrees	1896.47	517.47
In-plane, 90 degrees	108.7	517.47
Compression Ultimate Stress	MPa	MPa
In-plane, 0 degrees	1567.07	512.03
In-plane, 90 degrees	134.05	512.03
Shear Ultimate Stress	MPa	MPa
In-plane	63.08	279.36

The thickness of one layer of laminate is fixed at 0.022 inches (0.5588 mm). The face sheet thickness is specified as an input for the analysis. Therefore, the number of laminate layers is determined by the minimum number required to meet or exceed the specified face sheet thickness. Due to the fact that there are six shell sections and two face sheets (inner and outer) for each section, there can be at most twelve different values for the number of laminate layers. This can be reduced to six if the inner and outer face sheet values are made equal for each section. In addition to the shells, the beams are also made out of composites and assuming they are to be made in ply layers, then the same method applies to find the number of laminate layers. However, it is possible that some sections of the beam may have extra laminate layers for needed reinforcement. As for how these data are input into the finite element software, Appendices A and B have the information from the input files, also called the BDF files, and the cards and values that go into them. These are text files that Nastran reads and uses to develop the results for the given model. For the material and property values, the cards used are the MAT1, PCOMP, and PBARL cards (Nastran, 2006).

2.1.2 Phenolic Impregnated Carbon Ablator

In addition to the composite shell and support frame, there is another material that is placed on the outer surface of the structure to prevent significant heat transfer during entry into the Mars atmosphere. This material is known as the Thermal Protection System (TPS) which consists of Phenolic Impregnated Carbon Ablator (PICA) as well as a strain isolation pad (SIP) surrounded by room temperature vulcanizing (RTV) adhesive (Dwyer 2010). The role of this material is to insulate the structure from the heat load that is caused by the drag force against the atmosphere. The PICA material is designed to ablate in order to prevent heat from transferring to the load-carrying structure. In the finite element analysis software Nastran, this TPS material is considered to have nonstructural mass (NSM). This means that the mass from this material will not react to or absorb any of the structural loads applied during the analysis of the finite element model.

2.2 Nodes

For the development of the finite element model, the first step in the process is to create the nodes for the mesh; Appendix B.1 contains the GRID cards used to input the node locations into Nastran. The layout of the nodes consists of a single node at the top of the aeroshell followed by rings made up of a fixed number of nodes that are lined up along the entire length of the model. The initial design consisted of these rings of nodes being placed apart from each other at a fixed distance. However, the model needed to have nodes placed such that a finer mesh is developed in the top of the model. The reason for this is that for areas of a finite element model with more curvature, there is a higher chance that there will be large stresses in those regions. In order to predict those stresses accurately, there needs to be more elements. Thus, the distance between the rings of nodes in the top section decreases from the junction of the dome and cylinder to the top end of the dome. Figure 6 shows the layout of the nodes for the model. Notice the adjacent rings in the top section are closer in proximity to each other and that the adjacent ones in the cylinder are equidistant from each other.

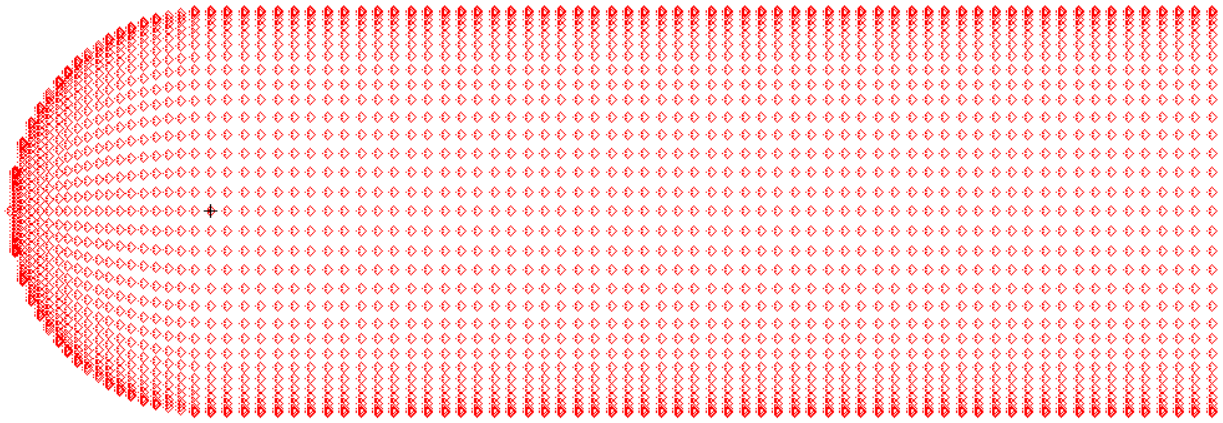

Figure 6. Finite Element Model - Nodes

2.3 Elements

After the nodal locations are defined, the elements are defined in the finite element model. The aeroshell consists of shell elements as well as bar elements that make up the support frame. In this project, the aim is to keep the model as simple as possible while maintaining reasonable accuracy. Thus, the shell of the structure is modeled using two-dimensional elements and the support frame beams are modeled using one-dimensional elements. More specifically, the shell is modeled using CTRIA3 and CQUAD4 elements, and the beams are modeled by CBAR elements. Appendix B.1 contains the list of these cards used to input the elements into Nastran. The CTRIA elements are triangular in shape and have nodes at the three vertices, and the CQUAD elements are rectangular in shape and have nodes at the four vertices. Almost all of the model is generated using CQUAD4 elements, but the top of the aeroshell is modeled with the CTRIA3 elements. The purpose of using triangular elements at the top of the model was to create a smooth and axisymmetric mesh on the entire model which can increase the accuracy of the results. Because the top of the model consists of only a single node, this symmetry could only be accomplished by using CTRIA elements in that location. In addition to these shell elements, there are a subset of CBAR elements that model the longerons which travel from the tip of the dome along the surface to the base. The rest of the CBAR elements travel circumferentially at fixed locations in the cylindrical part of the aeroshell and these rings of CBAR elements are equal distances from each other. Figure 7 shows the model with elements that represent the surface of the structure.

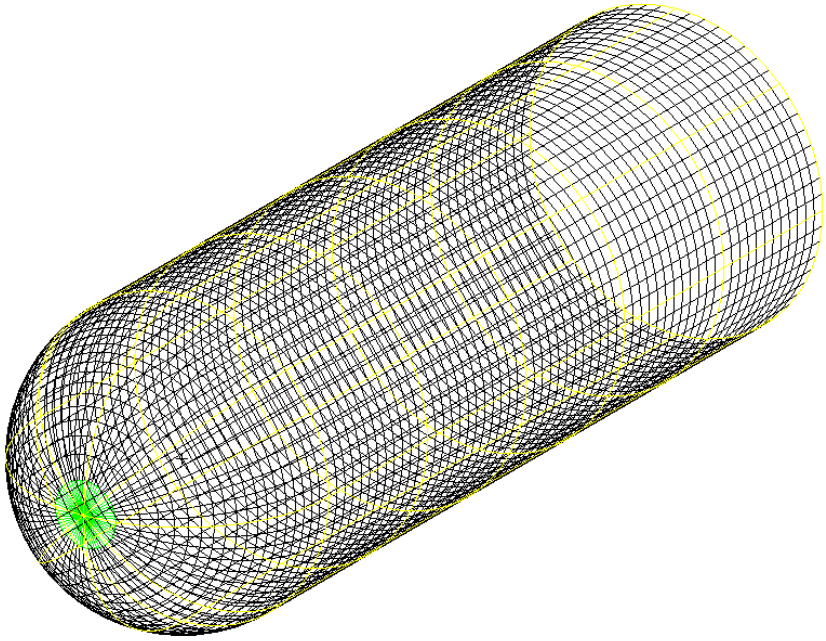

Figure 7. Finite Element Model - Elements

Each of these element types are given properties that define the shapes of the elements. The thickness defined for the CTRIA and CQUAD shell elements is symmetric about the initial two-dimensional surface from which the element originates. The properties for the CBAR beam elements include the cross section shape and the values for the different length dimensions of the cross section. Figure 8 shows images of the shell thickness from the model, Figure 9 shows images of the cross sections of the beam elements, and Figure 10 shows a diagram with the variable dimensions of the beam cross sections.

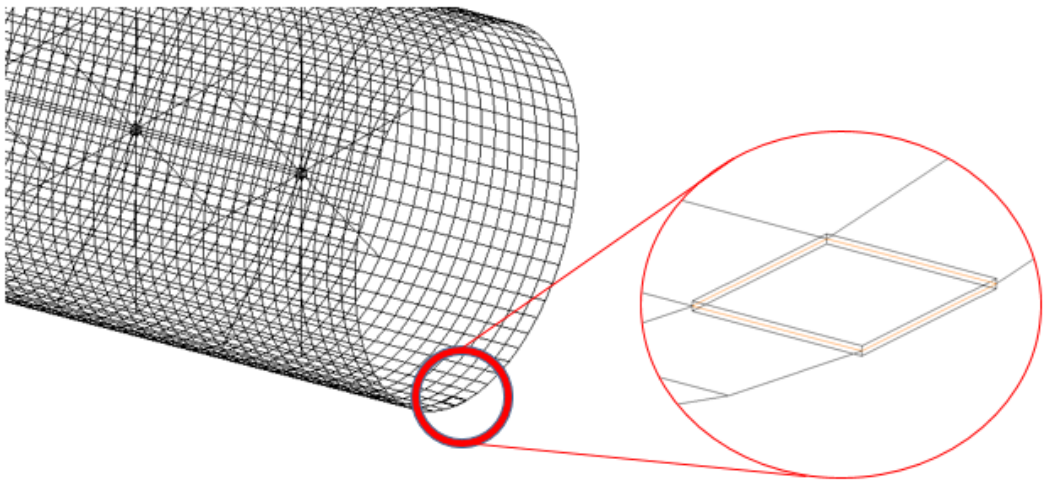

Figure 8. Shell Element

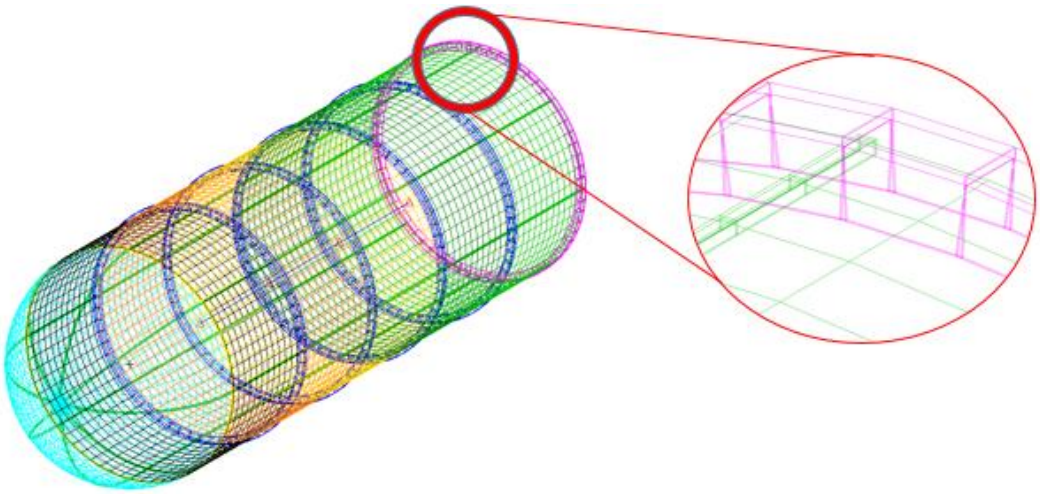

Figure 9. Beam Elements

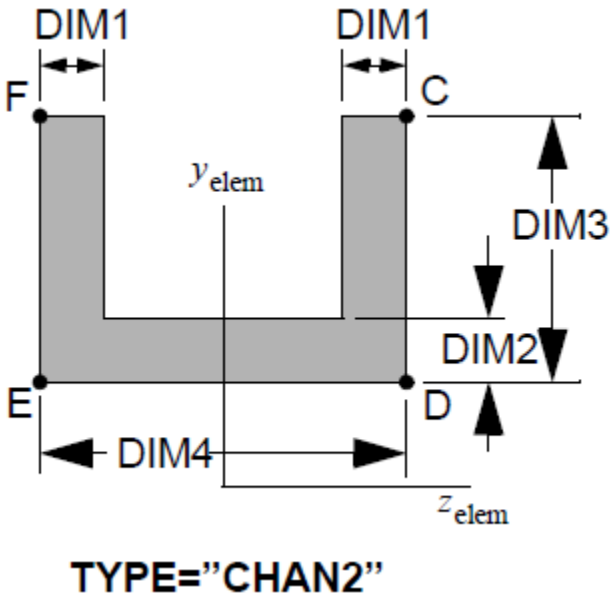

Figure 10. Beam Cross-Section Dimensions

In addition to the elements that model the surface, there are also elements included that model the payload that is attached to the aeroshell. The payload is modeled by four zero-dimensional point mass elements that are located in the cylinder part of the structure. These masses are attached to the aeroshell using multi-point constraint (MPC) markers which are RBE3 elements. These markers attach the mass elements to the nodes that are at the junctions between the inner frame rings and the longerons. In addition, the four masses are attached to each other

with CROD elements to account for the fact that each of these mass elements represent a part of the whole mass of the payload which is one single object. If they were not attached together, they would be allowed to move independently which would not provide an accurate model. These elements are only meant to be small links to the mass elements and should have no major impact in the analysis. The links are therefore given arbitrarily small values for their geometric dimensions to satisfy these conditions. The cross sectional area value is about 0.0025 m^2 which produces the radii value of about 0.03 m for the coefficient for torsional stress. These elements are also each assigned a torsional constant value of about 1.06e-6 m^4 which is calculated using Equation 1.

$$J = \frac{1}{2}\pi r^4 \tag{1}$$

Note that this equation is used for CROD elements with a uniform circular cross section where *r* is the radius for that cross section. Figure 11 shows the model with the masses, rods, and MPC markers added to it.

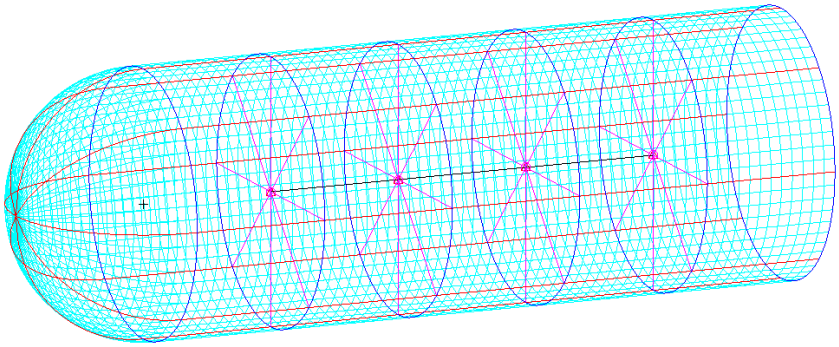

Figure 11. Payload Configuration

While the model may seem like it is only separated by the types of elements, it is actually divided even further due to the fact that groups of the elements are assigned with unique property identification (PID) numbers. While all the longerons have the same PID number, the shell elements are split by six PID numbers. The PID number that is assigned to a shell element is based on which of the six sections that shell element is in. The frames are also divided where the first frame has a unique PID number, the last frame has a unique PID number, and the rest of them all share a third PID number. This is to account for the fact that the inner frames need to be stronger since they are directly connected to the payload, and that the last frame also needs to be strong since it will be connected to the launch vehicle. Figure 3 shows the model with various colors to distinguish the differences in the elements based on the PID number assigned to them.

2.4 Loads and Boundary Conditions

For the loads and boundary conditions, there are two main groups to apply to the same structure that occur in different phases of the travel to Mars. The first step in the process is the launch of the structure from Earth. This transient period has a fair amount of pressure and some vibro-acoustic effects on the entire vehicle, and an appropriate analysis must be done to make sure that the structure is made such that it can handle the pressure and vibration associated with the rocket launch. In addition, the other stage that has a large impact is the entry into the Mars atmosphere. While there might not be any vibro-acoustic effects, there is still a high pressure and heat load during this phase.

2.4.1 Earth Launch Loads

The launch case consists of a few different loads and boundary conditions, where the most basic set is the static load case and the additional set is the vibro-acoustic load case. There are a few facts to note about the modeling of the launch. First, the aerodynamics are estimated by hypersonic theory (Lane 2017), though these estimates are not exact since most if not all of the launch consists of only subsonic and supersonic speed. Also, the rocket is not exactly vertical in its path out of the atmosphere, and as a result the model has been given an angle of attack of five degrees. Due to this non-zero angle, the pressure load is not only on the top end of the structure but also along the windward side of it.

For the boundary condition during the launch phase, the structure is modeled to represent the fact that it will be attached to the rocket at the base. Therefore the base has displacement constraints that prevent translational and rotational movement on that end. In addition, to represent the real constraint setup that would be applied to the aeroshell, the finite element model is constrained at the bottom but only at the junction of the longeron beam elements and last frame ring. Figure 12 shows the model with this boundary condition as well as additional constraints on the center reference node which prevent singularity issues during the analysis. Appendix B.1 shows the cards labeled SPC that represent these boundary conditions.

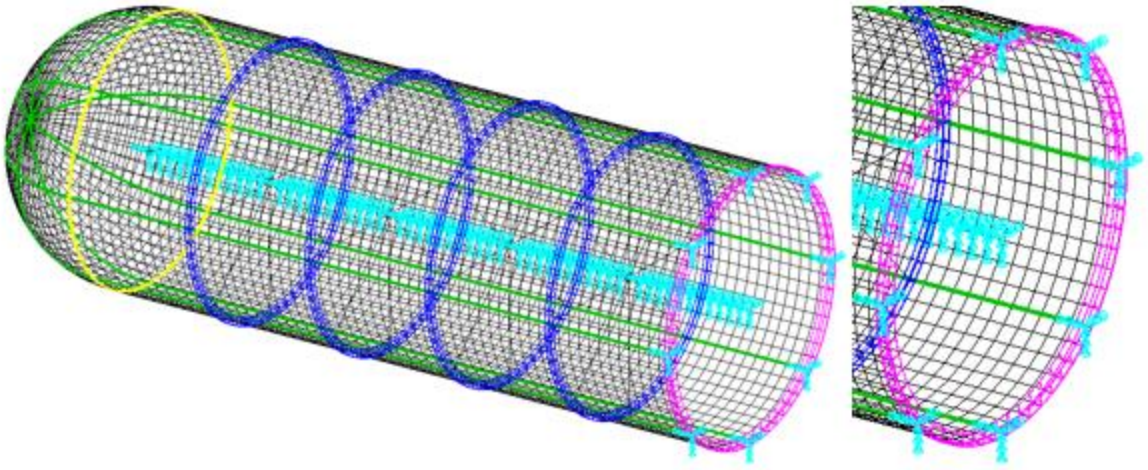

Figure 12. Boundary Condition

As for the loads in the static case, there are two different types: dynamic pressure and gravity. Appendix B.1 shows the cards labeled PLOAD4 and GRAV that represent these loads and the card LOAD that combines them into different load cases. For launch, aerodynamic pressure loads are not substantial when compared to gravity loads. Therefore, for this model they are present but minimal in magnitude with a maximum value of 2810 Pascals. Although there is not much data on the type of rocket that would take this structure into space, the g-loads during launch were estimated to be 4g in the axial direction and 0.75g in the lateral direction. These are suitable values for a launch that may potentially take humans into space since humans can only take a limited amount of g-load. Figure 13 shows the model with the boundary conditions as well as the pressure and gravity loads.

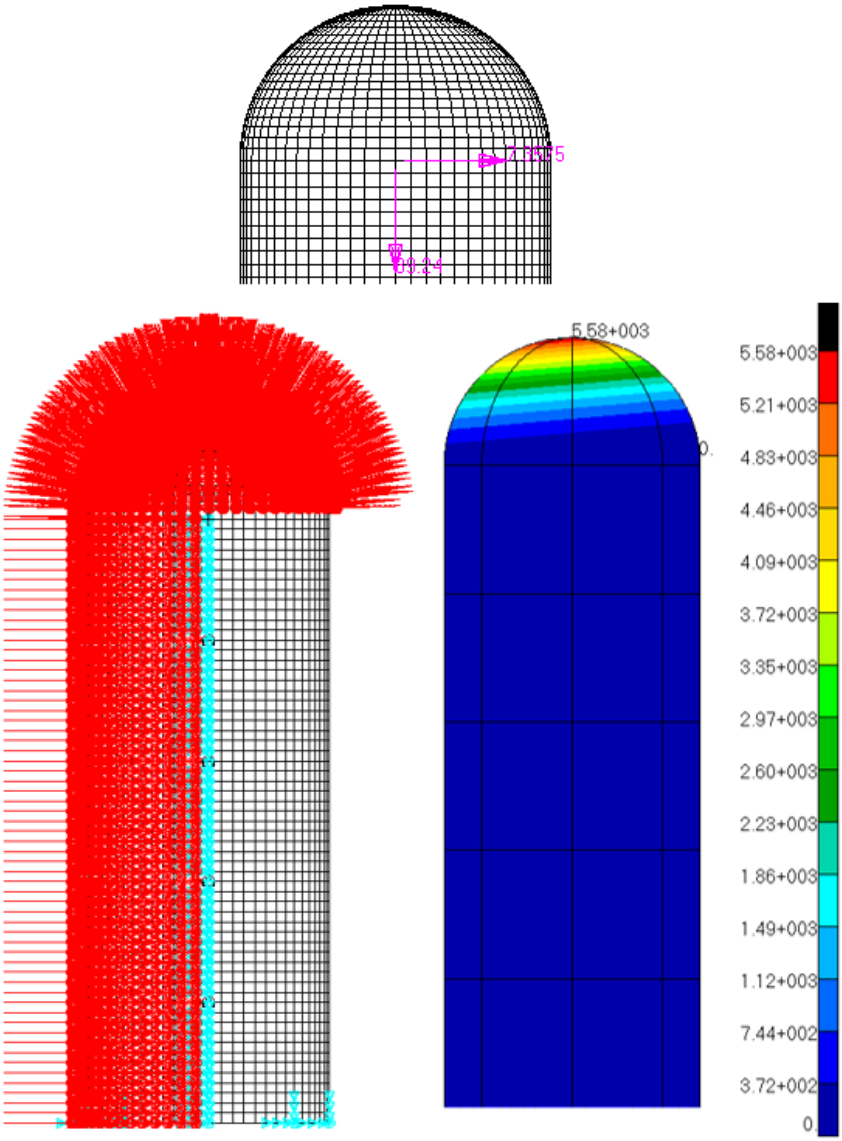

Figure 13. Earth Launch Load Case

In addition to the static load case, the launch of a rocket may produce some significant acoustic and vibration effects that may produce a problem for the rocket and its payload. Thus, there is also a vibro-acoustic analysis done in Nastran which takes a table of power spectral density and modal damping values and uses them in an analysis over a given frequency range. The results for this will be shown in a graph of the power spectral density of element stress over the frequency range. The actual stress value is the square root of the integral of the curve shown in the graph. Appendices A.2 and B.2 contain the input file data that are used to run the vibro-acoustic analysis.

2.4.2 Mars Entry Loads

The entry case only consists of one set of boundary conditions and loads. There are a few facts to note about the modeling of the entry into Mars. First, the aerodynamics when entering the Mars atmosphere are actually in the hypersonic speed range, so the hypersonic theory is relevant when determining the dynamic pressure values for this particular situation. In addition, a nonzero angle of attack leads to a pressure distribution on the top and along the windward side of the aeroshell. The angle of attack is fifty-five degrees during entry into Mars.

For the boundary conditions in the entry case, the model has to represent the fact that there are no physical constraints on the structure as it passes through the Mars atmosphere. Fortunately, Nastran has a method called Inertia Relief that can set up a model that has no physical boundary conditions for static analysis. Instead, the inertial characteristic of the mass in the model is used as the resistance against the applied loads which creates a configuration that puts the model in static equilibrium but still allows for rigid-body displacement.

For the loading of the entry case, only the pressure loads are present. For entry into the Mars atmosphere, the pressure plays a major role and thus is incorporated in the finite element model with a maximum value of 5000 Pascals. The reason why there are no explicit gravity loads is due to the fact that the inertia relief solution method balances the pressure load with the necessary gravity loads for static equilibrium. Figure 14 shows the model with the pressure loads, and Appendix B.1 shows the PLOAD4 cards that represent these loads and the LOAD card that creates the load case.

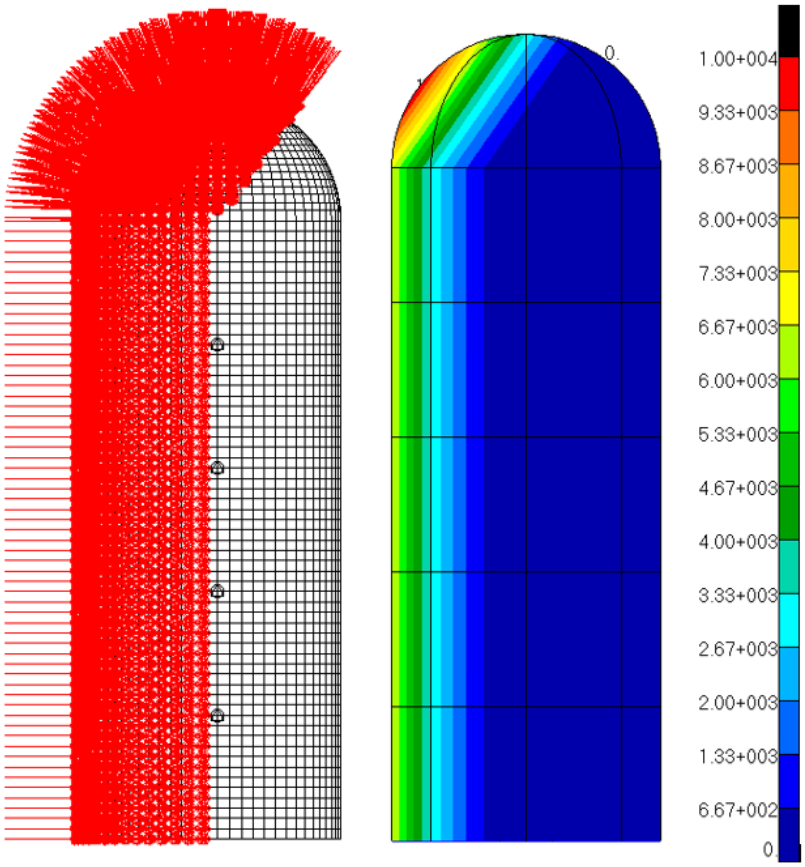

Figure 14. Mars Entry Load Case

3 Design Optimization

While the main optimization that is used to find the best model for this project is done using the program developed in Python for automated model generation and analysis (Lane 2017), each model with its unique set of parameter values goes through a smaller initial optimization process known as SOL 200 which is a solution used through Nastran. This solution method takes a given set of design variables and design constraints and attempts to find the optimal value for a certain design variable while staying within the region that does not violate any of the given design constraints (Moore, 1994). This optimal value can be a minimized or maximized value depending on what the user specifies. For example, the main variable to optimize in this project is the mass of the structure and the goal is to minimize it, so the solution would look for the smallest value for the mass of the aeroshell while trying to meet the user supplied constraints.

The constraints given in this analysis consist of several different types. The first set defines the geometric constraints on all of the shroud shell and beam elements. The constraints for the shell are broken up into the six sections and are separately defined for the composite

honeycomb core thicknesses and the laminate layer thicknesses. The constraints for the beams are defined the same for all of the longerons but are separate for each of the frame rings. These constraints limit all of the cross section dimensions for the beams that are shown in Figure 10. There are also a set of constraints for the ratios of the dimensions to ensure that the cross section geometry maintains its shape and does not result in overlapping segments. There is also a list of stress constraints used to make sure that the elements are optimized such that they can still handle the given stress requirements. The last large set of constraints are for buckling which are given the lower eigenvalue limit of 1.0 to prevent it from occurring. Finally, there is a single frequency constraint created to make sure that the structure does not experience any natural vibrations below the 7 Hertz requirement provided.

All of these values for the design optimization are put into the input file for Nastran to read, and all of the cards that hold these input values reside in the Bulk Data section of the input file. In addition, there is also the section of the input file known as the Case Control that references these data in the Bulk Data section in order to create different subcases to focus on different analysis types for the same set of data. For example, for each model in this design optimization, an analysis will be done to test for static loads, buckling, and normal modes which means there will be three subcases in one input file. The following subsections will explain these different components of the design optimization for the baseline model. Refer to the MD Nastran Quick Reference Guide (2006) to understand the formatting and the variables that each value is assigned to, and refer to Appendices A.3 and B.3 for the input file information for SOL 200.

3.1 Bulk Data section

The first type of Nastran card in the Bulk Data section that is crucial for the design optimization is the card called DESVAR. This card is used to give initial values to certain parameters such as length or cross-sectional area and also provide a range that the parameter values must stay within. In this project, these cards provide values for the thicknesses of the shell honeycomb core and face sheets as well as the value for the dimensions of the cross-sectional areas for the beam elements. These DESVAR cards are referenced by the cards called DVPREL1 which associate the initial values and ranges with the appropriate parameters from the property cards. For example, one of the DVPREL1 cards references the DIM1 value on the PBARL card which represents one of four cross-section dimensions and associates it with the proper DESVAR card that has an initial value of 0.0066701 m and a range of 0.005 – 0.04 m.

In addition to these inputs cards are the DRESP1 and DCONSTR cards which are used to set the limits for the constraints on certain variables. In the optimization for the aeroshell model, these cards restrict the values of the composite stress, beam stress, height-to-width ratios of beam dimensions (to prevent buckling), and acceptable values for the buckling modes and normal modes. To be more specific, the DRESP1 card signifies the attributes to be constrained and the DCONSTR card assigns the values for those constraints. For example, one parameter that needs to be set as an upper limit is the allowable stress of 512 MPa for the beam elements.

Thus, one DRESP1 card references the STRESS value for one of the PBARL cards and the DCONSTR sets the upper limit at 5.12E08 so that the stress level will not reach a value above the allowable stress where damage can occur. Note that while allowable stress is introduced, no factor of safety or knockdown factor was applied.

While most of the assigned values for the input cards are straightforward, the initial values on the DESVAR cards can have a significant impact on whether or not the solution leads to an optimized design, an infeasible design, or a feasible but non-optimized design. Unfortunately, there is no exact procedure to follow on what initial values to assign to the input cards in order to get the best results possible, and as the design becomes more complex it become harder to predict the combination of values that ought to be assigned to produce reasonable results. Through experimentation, it was found that in some cases the initial values could reduce or increase the mass by tens of thousands of kilograms which can be the difference between a viable or unacceptable design. At this point, experimentation is used to find values that would work and that would also produce acceptable optimized values.

3.2 Case Control Section

Initially there were two different case control sections: one for the Earth launch phase and one for the Mars entry phase. However, after running several preliminary design optimization tests, it was determined that the Earth launch load case is the driving load case and thus the only design optimization that is developed and performed is the one for this load case. In addition, the following explanation is only for the Case Control developed for the Earth launch load case.

The first input cards in the Case Control section are the following: the SOL 200 card to indicate the use of the design optimization solution, the DESOBJ card that signifies the DRESP1 card with the variable that is to be optimized which is mass in this case, and the ELSUM card that breaks down the mass components of the model to better determine which parts of the model are affected the most and if all the parts have mass values that make sense. After these are the cards for the different subcases. Each subcase is initialized with the line “SUBCASE #” and all of the cards associated with that subcase are indented after it. As was mentioned previously, there are three subcases to consider: statics, buckling, and normal modes. These analysis types are assigned within each subcase group with the input card ANALYSIS.

For the statics subcase, the physical constraints and pressure loads are referenced by the SPC and LOAD cards, respectively, and the DESSUB card references the DCONSTR cards that constrain the stress values. For the buckling subcase, the same physical constraints are referenced, but the DESSUB references DCONSTR cards that constrain the eigenvalues for buckling. This subcase also uses the METHOD card to reference an EIGRL card that defines how many roots are desired from the analysis. The last subcase references the same physical constraints and number of eigenvalue roots desired, but the DESSUB refers to one DCONSTR card that limits the frequency range of the normal modes. All of these subcases are optimized for as a collective whole in the same run, so the resulting values are such that the stress values fall

under the allowable stress, buckling is prevented from occurring, and the lowest normal modes maintain values at or above the lower limit provided. If these subcases were not all included then the resulting values would not satisfy all of the subcases, so it is crucial that all three of these subcases are included in all the design optimizations that are performed.

4 Results and Discussion

4.1 Design Optimization

Before running the analysis to find the resulting deformation and stress values, a design optimization will be run so that optimal values for the parameters and dimensions can be obtained which should result in better values from the subsequent analyses. As mentioned in Section 4.2, due to the fact that it was found that the Earth launch load case was the driving factor for the optimization, only the results for the Earth launch load case will be sought since they will produce values that must be used over the values that any Mars Entry optimization would produce. Table 4 shows the results taken directly from a Nastran results file, also known as the F06 file, for an optimization of statics, buckling, and normal modes. These results consist of the final values for the overall mass, the thicknesses of the shell honeycomb cores and face sheets, and the beam cross-section dimensions for the single set of longerons and for the three groups of frame rings. While the primary and most important design optimization consists of the static, buckling, and normal mode analysis subcases all combined under the same run, other design optimizations have been run with different combinations of the subcases in order to show which subcase has the biggest impact on the optimization of the finite element model. Table 5 shows the results from this design optimization where all three subcases are incorporated in the same run, but it also includes the results from runs composed of different combinations of the same subcases. Table 6 shows the number of laminate layers needed for the optimized thicknesses of the face sheets.

Table 4. Design Optimization Final Results

----- DESIGN OBJECTIVE -----

INTERNAL RESPONSE ID	DRESPx	RESPONSE TYPE	MINIMIZE OR MAXIMIZE	SUPERELEMENT ID	SUBCASE ID	VALUE
1	DRESP1	WEIGHT	MINIMIZE	0	0	1.3840E+05

----- DESIGN VARIABLES -----

INTERNAL ID	DESVAR ID	LABEL	LOWER BOUND	VALUE	UPPER BOUND
1	1	CORE_0	1.0000E-02	1.0000E-02	1.0000E-01
2	2	LAM_0	1.0000E-03	1.0000E-03	2.0000E-02
3	3	CORE_1	1.0000E-02	1.0000E-02	1.0000E-01
4	4	LAM_1	1.0000E-03	1.0000E-03	2.0000E-02
5	5	CORE_2	1.0000E-02	1.6679E-02	1.0000E-01
6	6	LAM_2	1.0000E-03	4.4069E-03	2.0000E-02
7	7	CORE_3	1.0000E-02	1.5505E-02	1.0000E-01
8	8	LAM_3	1.0000E-03	8.8445E-03	2.0000E-02
9	9	CORE_4	1.0000E-02	1.4878E-02	1.0000E-01
10	10	LAM_4	1.0000E-03	1.3690E-02	2.0000E-02
11	11	CORE_5	1.0000E-02	4.7380E-02	1.0000E-01
12	12	LAM_5	1.0000E-03	2.0000E-02	2.0000E-02
13	13	LDIM1	5.0000E-03	6.6701E-03	4.0000E-02
14	14	LDIM2	5.0000E-03	8.8865E-03	4.0000E-02
15	15	LDIM3	5.0000E-02	5.5141E-02	3.0000E-01
16	16	LDIM4	5.0000E-02	7.1586E-02	3.0000E-01
17	17	FDIM1_0	5.0000E-03	7.2810E-03	4.0000E-02
18	18	FDIM2_0	5.0000E-03	9.8626E-03	4.0000E-02
19	19	FDIM3_0	4.0000E-02	5.9649E-02	3.0000E-01
20	20	FDIM4_0	4.0000E-02	8.1064E-02	3.0000E-01
21	21	FDIM1_1	5.0000E-03	1.0747E-02	4.0000E-02
22	22	FDIM2_1	5.0000E-03	1.4367E-02	4.0000E-02
23	23	FDIM3_1	4.0000E-02	3.0000E-01	3.0000E-01
24	24	FDIM4_1	4.0000E-02	1.5718E-01	3.0000E-01
25	25	FDIM1_2	5.0000E-03	1.0765E-02	4.0000E-02
26	26	FDIM2_2	5.0000E-03	3.7500E-02	4.0000E-02
27	27	FDIM3_2	4.0000E-02	3.0000E-01	3.0000E-01
28	28	FDIM4_2	4.0000E-02	3.0000E-01	3.0000E-01

Table 5. Design Optimization Comparison of Results

Design Optimization with Baseline Model	Earth Launch					
	Initial Values	Statics	Statics & Buckling	Modes	Statics & Modes	All Subcases
OPTIMUM AT CYCLE NUMBER.....	N/A	5	6	8	8	8
MASS (kg)						
Total mass	2.0026E+05	1.1363E+05	1.1366E+05	1.3845E+05	1.3840E+05	1.3840E+05
Structural mass	1.9103E+05	1.0440E+05	1.0443E+05	1.2921E+05	1.2917E+05	1.2917E+05
Aeroshell mass	9.1030E+04	4.4000E+03	4.4300E+03	2.9210E+04	2.9170E+04	2.9170E+04
Aeroshell aerial density	8.2788E+01	4.0016E+00	4.0289E+00	2.6565E+01	2.6529E+01	2.6529E+01
DIMENSIONS (m)						
Core upper limit	1.0000E-01	1.0000E-01	1.0000E-01	1.0000E-01	1.0000E-01	1.0000E-01
Core lower limit	1.0000E-02	1.0000E-02	1.0000E-02	1.0000E-02	1.0000E-02	1.0000E-02
Laminate upper limit	2.0000E-02	2.0000E-02	2.0000E-02	2.0000E-02	2.0000E-02	2.0000E-02
Laminate lower limit	1.0000E-03	1.0000E-03	1.0000E-03	1.0000E-03	1.0000E-03	1.0000E-03
CORE_0	1.0000E-01	1.0000E-02	1.0000E-02	1.0000E-02	1.0000E-02	1.0000E-02
LAM_0	2.0000E-02	1.0000E-03	1.0000E-03	1.0000E-03	1.0000E-03	1.0000E-03
CORE_1	1.0000E-01	1.0000E-02	1.0000E-02	1.0000E-02	1.0000E-02	1.0000E-02
LAM_1	2.0000E-02	1.0000E-03	1.0000E-03	1.0000E-03	1.0000E-03	1.0000E-03
CORE_2	1.0000E-01	1.0000E-02	1.0000E-02	1.9588E-02	1.6679E-02	1.6679E-02
LAM_2	2.0000E-02	1.0000E-03	1.0000E-03	4.3145E-03	4.4069E-03	4.4069E-03
CORE_3	1.0000E-01	1.0000E-02	1.0000E-02	1.8682E-02	1.5505E-02	1.5505E-02
LAM_3	2.0000E-02	1.0000E-03	1.0000E-03	8.6104E-03	8.8445E-03	8.8445E-03
CORE_4	1.0000E-01	1.0000E-02	1.0000E-02	1.8451E-02	1.4878E-02	1.4878E-02
LAM_4	2.0000E-02	1.0000E-03	1.0000E-03	1.3634E-02	1.3690E-02	1.3690E-02
CORE_5	1.0000E-01	1.0000E-02	1.1645E-02	4.7028E-02	4.7380E-02	4.7380E-02
LAM_5	2.0000E-02	1.0000E-03	1.0000E-03	2.0000E-02	2.0000E-02	2.0000E-02
DIM1 & DIM2 upper bound	4.0000E-02	4.0000E-02	4.0000E-02	4.0000E-02	4.0000E-02	4.0000E-02
DIM1 & DIM2 lower bound	5.0000E-03	5.0000E-03	5.0000E-03	5.0000E-03	5.0000E-03	5.0000E-03
DIM3 & DIM4 upper bound	3.0000E-01	3.0000E-01	3.0000E-01	3.0000E-01	3.0000E-01	3.0000E-01
DIM3 & DIM4 lower bound	5.0000E-02	5.0000E-02	5.0000E-02	5.0000E-02	5.0000E-02	5.0000E-02
LDIM1	4.0000E-02	5.0000E-03	5.0000E-03	7.4195E-03	6.6701E-03	6.6701E-03
LDIM2	4.0000E-02	5.0000E-03	5.0000E-03	1.0410E-02	8.8865E-03	8.8865E-03
LDIM3	3.0000E-01	5.0000E-02	5.0004E-02	5.4563E-02	5.5141E-02	5.5141E-02
LDIM4	3.0000E-01	5.0000E-02	5.0000E-02	6.9201E-02	7.1586E-02	7.1586E-02
FDIM1_0	2.0000E-02	5.0000E-03	5.0000E-03	9.6391E-03	7.2810E-03	7.2810E-03
FDIM2_0	2.0000E-02	5.0000E-03	5.0000E-03	1.2749E-02	9.8626E-03	9.8626E-03
FDIM3_0	1.5000E-01	4.0000E-02	4.0000E-02	6.1976E-02	5.9649E-02	5.9649E-02
FDIM4_0	1.5000E-01	4.0000E-02	4.0000E-02	8.2255E-02	8.1064E-02	8.1064E-02
FDIM1_1	4.0000E-02	5.0000E-03	5.0000E-03	1.0037E-02	1.0747E-02	1.0747E-02
FDIM2_1	4.0000E-02	5.0000E-03	5.0000E-03	1.7269E-02	1.4367E-02	1.4367E-02
FDIM3_1	3.0000E-01	4.0000E-02	4.0000E-02	3.0000E-01	3.0000E-01	3.0000E-01
FDIM4_1	3.0000E-01	4.0000E-02	4.0000E-02	1.3453E-01	1.5718E-01	1.5718E-01
FDIM1_2	4.0000E-02	5.0000E-03	5.0000E-03	1.4649E-02	1.0765E-02	1.0765E-02
FDIM2_2	4.0000E-02	5.0000E-03	5.0017E-03	4.0000E-02	3.7500E-02	3.7500E-02
FDIM3_2	3.0000E-01	4.0000E-02	9.6623E-02	2.7506E-01	3.0000E-01	3.0000E-01
FDIM4_2	3.0000E-01	4.0000E-02	8.6044E-02	3.0000E-01	3.0000E-01	3.0000E-01

Note: F_0 = First/Top Frame F_1 = Support Frames F_2 = Last/Bottom Frame

Note: Color gradients only compare values in the same row

Table 6. Laminate Layers

All Subcases - # of laminate layers in one of the two face sheet in each section					
LAM_0	LAM_1	LAM_2	LAM_3	LAM_4	LAM_5
2	2	8	16	25	36

4.1.1 Impact of each subcase

The overall pattern of the values in Table 5 show that when compared to the initial values, all of the design optimizations result in the reduction of most if not all of the values which is a good sign that the optimization functions properly. However, the more important aspect to look at is the comparison of the values of the runs to each other. One point of interest is that the runs of the Static and Statics & Buckling significantly reduce the values of all of the variables which indicates that they are not a major source for the thickening of any of the shell sections or beams. It is only with the runs that include the normal modes analysis that a sharp increase in the values occurs which concludes that the normal mode analysis is the driving force that determines how large the values for the dimensions will be. Another set of comparisons in Table 5 that supports this conclusion is that the values between the runs Modes and Statics & Modes changes but not by much, and the values between the runs Statics & Modes and All Subcases barely change at all. This shows that adding in Statics impacts the values by a small amount compared to Modes, and adding in Buckling does almost nothing to change the values. While these results indicate that buckling may be of little importance that it can be taken out of the analysis completely, keeping it in the design optimization ensures that the model is optimized with the consideration of buckling included. Table 7 is the proof from the F06 file that the buckling criteria was met. All of the values in the Eigenvalue column are above the value 1 which indicates that no buckling occurs in the structure under the given loads. In addition to that, Table 8 is the proof that the modal expectation was met as well. All of the values in the Cycles column are roughly at or above 7 Hertz which means that the aeroshell will not experience any natural vibrations at frequencies below 7 Hertz.

Table 7: Results for Buckling

E I G E N V A L U E A N A L Y S I S S U M M A R Y (READ MODULE)

SUBCASE 2

R E A L E I G E N V A L U E S

MODE NO.	EXTRACTION ORDER	EIGENVALUE	RADIANS	CYCLES	GENERALIZED MASS	GENERALIZED STIFFNESS
1	1	2.355887E+01	4.853748E+00	7.724980E-01	3.230432E+06	7.610533E+07
2	2	2.727356E+01	5.222409E+00	8.311722E-01	1.122134E+07	3.060458E+08
3	3	2.728231E+01	5.223247E+00	8.313056E-01	1.115277E+07	3.042733E+08
4	4	3.717193E+01	6.096879E+00	9.703484E-01	2.461860E+06	9.151210E+07
5	5	3.792508E+01	6.158334E+00	9.801293E-01	8.582651E+04	3.254977E+06
6	6	3.796570E+01	6.161632E+00	9.806541E-01	8.617092E+04	3.271540E+06
7	7	3.807476E+01	6.170475E+00	9.820616E-01	6.675110E+04	2.541532E+06
8	8	3.807505E+01	6.170498E+00	9.820653E-01	7.438178E+04	2.832090E+06
9	9	3.833303E+01	6.191368E+00	9.853868E-01	1.424279E+05	5.459692E+06
10	10	3.835067E+01	6.192792E+00	9.856134E-01	1.468917E+05	5.633395E+06

Table 8: Results for Normal Modes

E I G E N V A L U E A N A L Y S I S S U M M A R Y (READ MODULE)

SUBCASE 3

R E A L E I G E N V A L U E S

(BEFORE AUGMENTATION OF RESIDUAL VECTORS)

MODE NO.	EXTRACTION ORDER	EIGENVALUE	RADIANS	CYCLES	GENERALIZED MASS	GENERALIZED STIFFNESS
1	1	1.924766E+03	4.387216E+01	6.982471E+00	1.000000E+00	1.924766E+03
2	2	1.924766E+03	4.387216E+01	6.982471E+00	1.000000E+00	1.924766E+03
3	3	5.163802E+03	7.185960E+01	1.143681E+01	1.000000E+00	5.163802E+03
4	4	5.163802E+03	7.185960E+01	1.143681E+01	1.000000E+00	5.163802E+03
5	5	5.778389E+03	7.601572E+01	1.209828E+01	1.000000E+00	5.778389E+03
6	6	5.778389E+03	7.601572E+01	1.209828E+01	1.000000E+00	5.778389E+03
7	7	1.244237E+04	1.115454E+02	1.775300E+01	1.000000E+00	1.244237E+04
8	8	1.249880E+04	1.117980E+02	1.779321E+01	1.000000E+00	1.249880E+04
9	9	1.308648E+04	1.143962E+02	1.820672E+01	1.000000E+00	1.308648E+04
10	10	1.308648E+04	1.143962E+02	1.820672E+01	1.000000E+00	1.308648E+04

4.1.2 Legitimacy of results

In addition to getting results that satisfy the design optimization, careful examination must be made with the output values to make sure that they make sense and that the right values are changing in the right directions. From the look of the values in the last column in Table 5, it seems that the values are increasing or decreasing as expected. First, the larger beam dimensions are greater than the shell thicknesses which is a good sign that the beams are taking the majority of the applied load as they are supposed to. Second, for both the shell sections and frame rings, the values of the sections or groups that are closer to the bottom are larger in magnitude compared to the ones at the top of the model. This indicates the shells and beams near the bottom have more mass on top of them and thus must support more load than just the applied pressure. Not only that, but based on preliminary analyses that were run, the top of the model has the most deformation when looking at the lowest modal frequencies, and a good way to counteract that motion is to make the bottom end more rigid to prevent the lateral swaying motion that is seen with the lowest two frequency modes.

Not only should the dimensions be checked for validity, but the mass values for each part of the model should also be checked to make sure nothing seems way out of proportion. Fortunately, the F06 file provides an Element Property Summary which shows the mass breakdown for the entire model. This table of values can be obtain with the Nastran card ELSUM(PIDSUM) used in the Case Control section of the design optimization BDF file as shown in Appendix A.3. This table of mass value is shown in Table 9 and has the mass components broken into three major categories: structural mass, non-structural mass, total mass. Note that there is a fourth category, but because our density values are all based on mass and not weight, the values in that column are exactly the same as the total mass values. Also note that the structural mass is the most important type in this project as this is the mass that is being reduced through the design optimization and parametric study.

Table 9: Mass Breakdown

E L E M E N T P R O P E R T Y S U M M A R Y (BY PROPERTY TYPE / ID)

				STRUCT.MASS	NON-STR.MASS	TOTAL MASS	TM*WTMASS
SUBTOTAL MASS FOR ALL BAR	ELEMENTS	FOR PBARL, ID =	20000	5.2036E+02	0.0000E+00	5.2036E+02	5.2036E+02
SUBTOTAL MASS FOR ALL BAR	ELEMENTS	FOR PBARL, ID =	22000	7.5641E+01	0.0000E+00	7.5641E+01	7.5641E+01
SUBTOTAL MASS FOR ALL BAR	ELEMENTS	FOR PBARL, ID =	22001	1.6666E+03	0.0000E+00	1.6666E+03	1.6666E+03
SUBTOTAL MASS FOR ALL BAR	ELEMENTS	FOR PBARL, ID =	22002	8.3861E+02	0.0000E+00	8.3861E+02	8.3861E+02
SUBTOTAL MASS FOR ALL BAR	ELEMENTS			3.1012E+03	0.0000E+00	3.1012E+03	3.1012E+03
SUBTOTAL MASS FOR ALL CONM2	ELEMENTS			1.0000E+05	0.0000E+00	1.0000E+05	1.0000E+05
SUBTOTAL MASS FOR ALL SHELL	ELEMENTS	FOR PCOMP, ID =	30000	6.5105E+02	1.5369E+03	2.1879E+03	2.1879E+03
SUBTOTAL MASS FOR ALL SHELL	ELEMENTS	FOR PCOMP, ID =	30001	6.5185E+02	1.5388E+03	2.1906E+03	2.1906E+03
SUBTOTAL MASS FOR ALL SHELL	ELEMENTS	FOR PCOMP, ID =	30002	2.4463E+03	1.5388E+03	3.9850E+03	3.9850E+03
SUBTOTAL MASS FOR ALL SHELL	ELEMENTS	FOR PCOMP, ID =	30003	4.6298E+03	1.5388E+03	6.1685E+03	6.1685E+03
SUBTOTAL MASS FOR ALL SHELL	ELEMENTS	FOR PCOMP, ID =	30004	7.0243E+03	1.5388E+03	8.5631E+03	8.5631E+03
SUBTOTAL MASS FOR ALL SHELL	ELEMENTS	FOR PCOMP, ID =	30005	1.0661E+04	1.5388E+03	1.2200E+04	1.2200E+04
SUBTOTAL MASS FOR ALL SHELL	ELEMENTS			2.6064E+04	9.2307E+03	3.5295E+04	3.5295E+04
SUBTOTAL MASS FOR ALL QUAD4	ELEMENTS			2.6051E+04	9.1982E+03	3.5249E+04	3.5249E+04
SUBTOTAL MASS FOR ALL TRIA3	ELEMENTS			1.3740E+01	3.2435E+01	4.6175E+01	4.6175E+01
SUBTOTAL MASS FOR ALL ROD	ELEMENTS	FOR PROD, ID =	10000	0.0000E+00	0.0000E+00	0.0000E+00	0.0000E+00
SUBTOTAL MASS FOR ALL ROD	ELEMENTS			0.0000E+00	0.0000E+00	0.0000E+00	0.0000E+00
TOTAL MASS FOR ALL SUPPORTED ELEMENT TYPES				1.2917E+05	9.2307E+03	1.3840E+05	1.3840E+05

When examining the values of the structure mass components relative to each other, it seems that the elements have mass values that are reasonable. Both the shell mass and beam mass values increase in the element groups that are closer to the bottom of the model, which makes sense as was explained earlier in this section. In addition to that, the CONM2 which represents the payload has the value of 100,000 kg which was the exact value assigned to it.

Also, the shell mass is greater than the beam mass due to the fact that there is more shell material, and the structural mass is much greater than the non-structural mass which should be the case since there is more metal and composite material compared to the amount of material for the TPS.

Another method used to verify the validity of these results is to perform simple hand calculations to see if the same values are obtained as those shown in the output file. To start with, Equation 2 is used to calculate the total amount of non-structural mass. Note that *D* is the aeroshell diameter, $L_{cylinder}$ is the aeroshell cylinder diameter, and ρ_{TPS} is the density of the Thermal Protection System. Using it along with the values for the baseline model produces a value of 9236.28 kg which gives an error of 0.06% from the value given by Nastran.

$$mass\ (kg) = \left[2\pi * \frac{D}{2} + \ \pi * D * L_{cylinder}\right] * \rho_{TPS} \tag{2}$$

Next is Equation 3 which is used to calculate the total mass of the longerons for the baseline model. Note that ρ_{beam} is the beam density, and the *DIM* variables are the dimensions from Figure 10. With the baseline model values substituted into the equation, it gives a value of 520.42 kg which is nearly identical to the value from Nastran.

$$total\ mass\ (kg) = 8 * \rho_{beam} * \left(L_{cylinder} + \frac{D}{2} * \frac{\pi}{2}\right) * [DIM4 * DIM2 + 2 * DIM1 * (DIM3 - DIM2)] \tag{3}$$

Next is Equation 4 which is used for the frame rings. The equation will be used to test the value for the very top frame ring, which shows a hand-calculated value of 75.67 kg. This value is also nearly identical to the value given by Nastran.

$$mass\ (kg) = \ \rho_{beam} * D * \pi * [DIM4 * DIM2 + 2 * DIM1 * (DIM3 - DIM2)] \tag{4}$$

Finally, there is Equation 5 which is the equation for the shell mass for one section only. Note that t_{CORE} and t_{LAM} are the thicknesses for the core and laminate layers, respectively, and ρ_{CORE} and ρ_{LAM} are the densities for the core and laminate layers, respectively. This equation results in a value for shell section one of 652.11 kg which is only one kilogram different from the value from the F06 file.

$$\frac{1}{5} * L_{cylinder} * D * \pi * 2 * (t_{CORE} * \rho_{CORE} + t_{LAM} * \rho_{LAM}) \tag{5}$$

4.1.3 Visual results

The numerical results from this analysis are imported into Patran and the visual results can be displayed to get a physical picture of how all the beams and shells relate to each other. Figure 15 shows the overall structure as well as close-up views of the frame rings to see the distinct size from each group. Just like the numerical results, the image shows the beam becoming thicker near the bottom. Similarly, Figure 16 shows contours that represent the values of the shell thickness. The dark blue at the top indicate the smallest values, the lighter shades of blue indicate that the thickness is greater compared to the top, and the red at the bottom represents the thickest values. Just like the numerical results, the image shows the thickness increase closer to the bottom of the model.

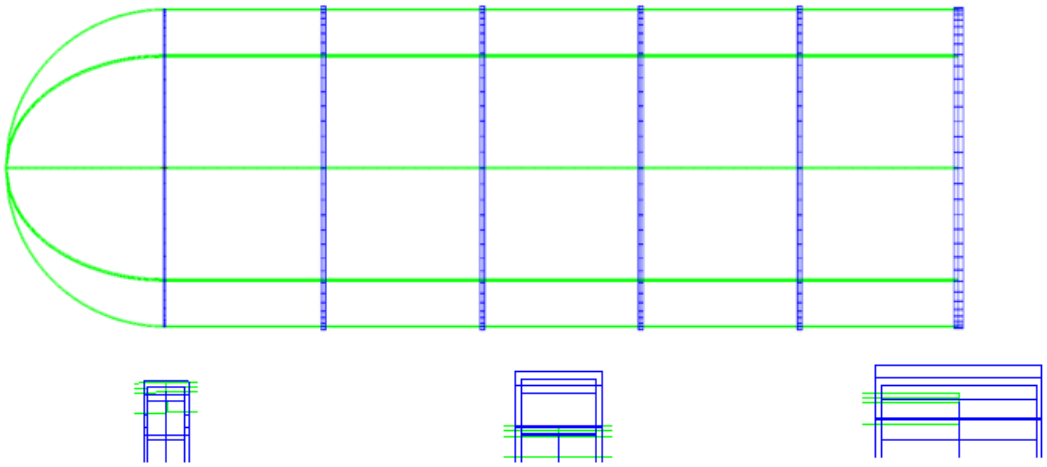

Figure 15. Variation in Support Frame

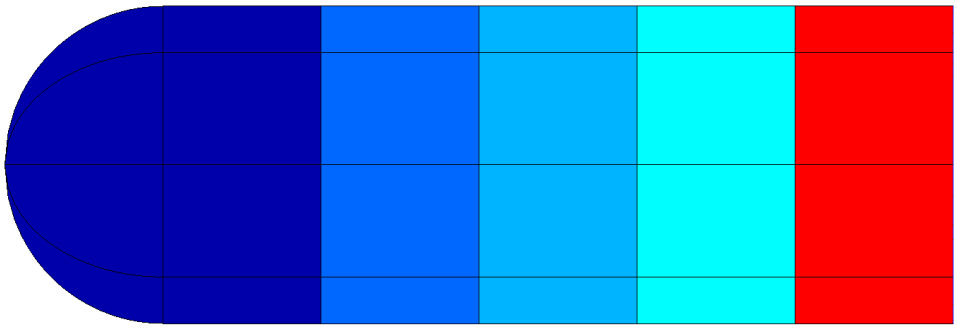

Figure 16. Variation in Shell Section

In addition to these visual results, Figure 17 gives the image of the model with the location of the center of gravity. This is shown just for reference to get an idea of where this value is located on the model. According to the numerical results that Patran shows with this image, the center of gravity is located 18.21 meters below the top of the model, or 13.21 meters below the top of the cylinder section. This is more than half way down the model which makes sense since the bottom is heavier which will shift the center of gravity towards the bottom of the model. In addition, the numerical results also indicates that the model has a total mass of 138 400 kilograms (which agrees with the F06 file) and that the material of the model takes up a volumetric space of 53.27 cubic meters.

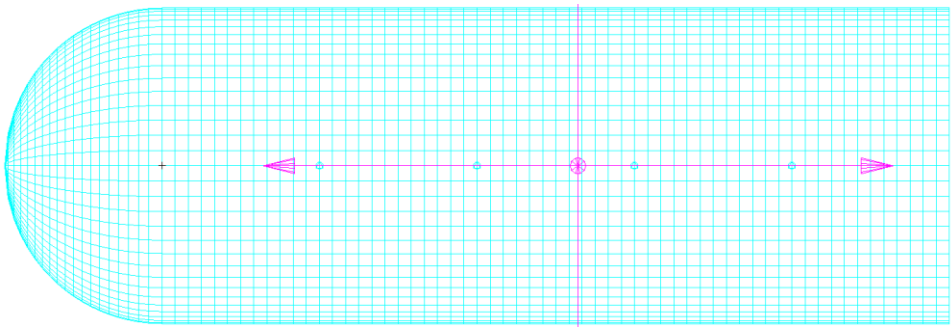

Figure 17. Location of Center of Gravity

4.2 Mars Entry Case

4.2.1 Statics

While the Mars entry case is not the driving case for the entire analysis, the results will still be shown in this report both for completeness and to explicitly verify that all the requirements for the Mars entry case are met. To start with, the deformation results for the static analysis are shown in Figure 18 to give a good idea about how the model physically reacts to the loads. Note that these deformations are exaggerated to make it easier to see them. Also note that the label “front” refers to the side that is facing the windward direction, the label “back” indicates the opposite side leeward, and the label “side” refers to the view that is perpendicular to the windward direction.

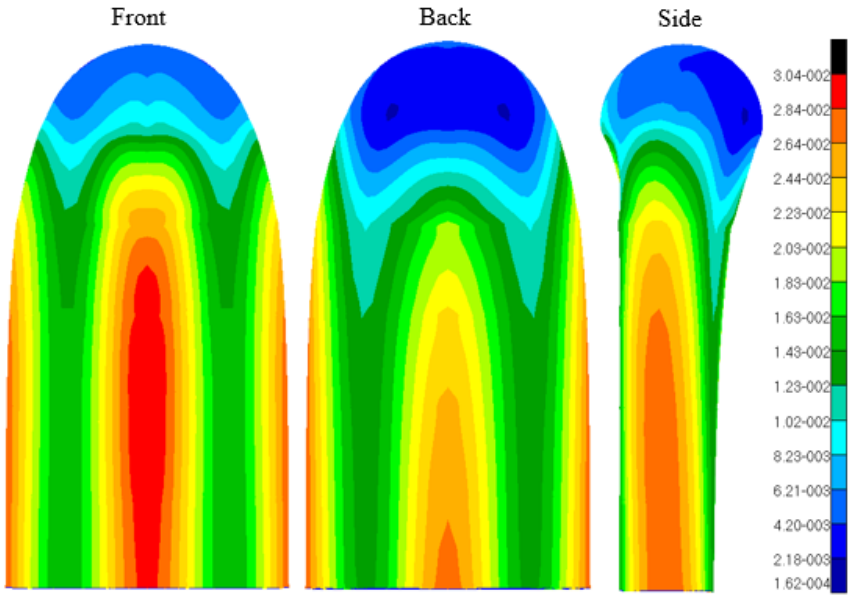

Figure 18. Mars Entry Deformation Contour

This image shows that the dome essentially stays in its initial shape whereas the middle of the cylinder section caves into the hollow space inside the model, though only by a few centimeters. So overall, this plot shows acceptable results devoid of any major deformation. In addition to this is Figure 19 which displays the contours for the maximum bar stresses which is the summation of the axial and bending bar stresses.

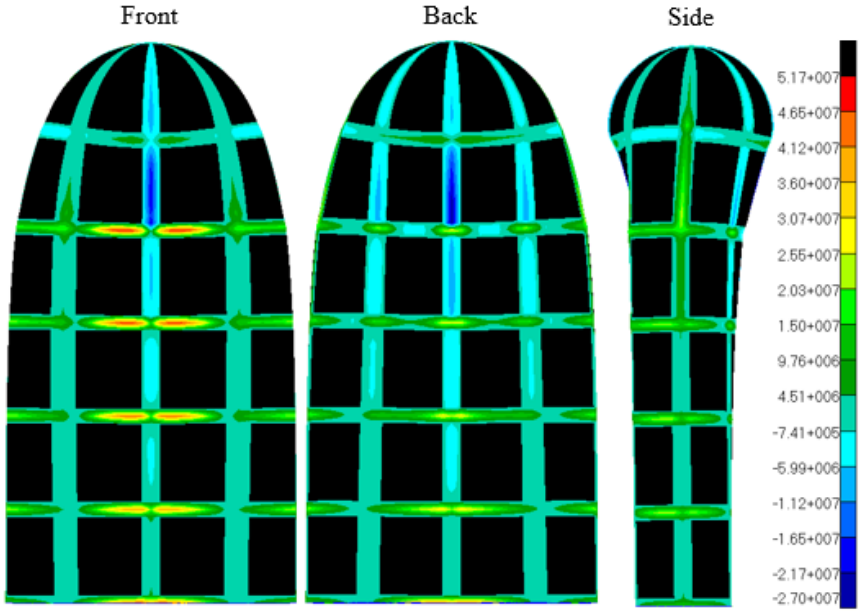

Figure 19. Mars Entry Bar Stress Contour

Based on the input data shown in the shell material table in the Materials section, the allowable stress requirement is 512 MPa. The results in the image show a maximum value of 51.7 MPa, so the bar stress values are within the acceptable range. Lastly and most importantly are the contour plots of the major principal stresses. There are technically four different plots for the four layers of the composite shell (the two face sheets and the honeycomb core split into equal halves), but only two plots will be shown where one displays the face sheet with the higher maximum principal stresses and the other displays the honeycomb core section with the higher maximum principal stresses. In this particular case, the inner honeycomb core and the inner face sheet sections have the higher maximum principal stress which are shown in Figure 20 and Figure 21, respectively.

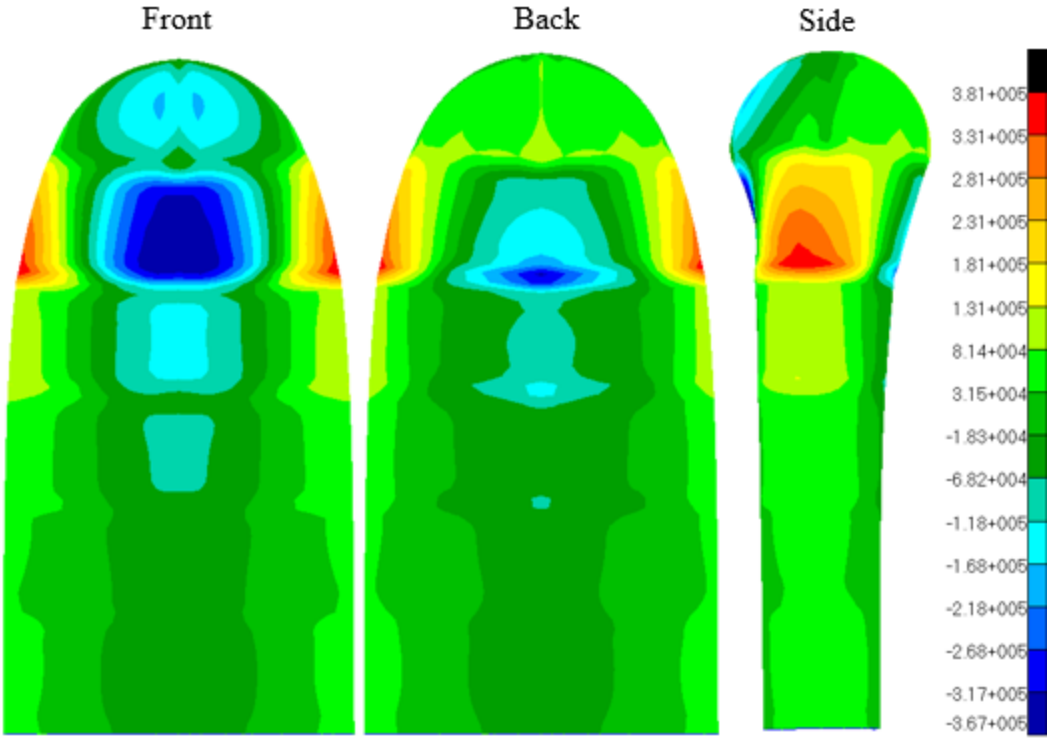

Figure 20. Mars Entry Maximum Principal Stress Contours for Honeycomb Core (Layer 3)

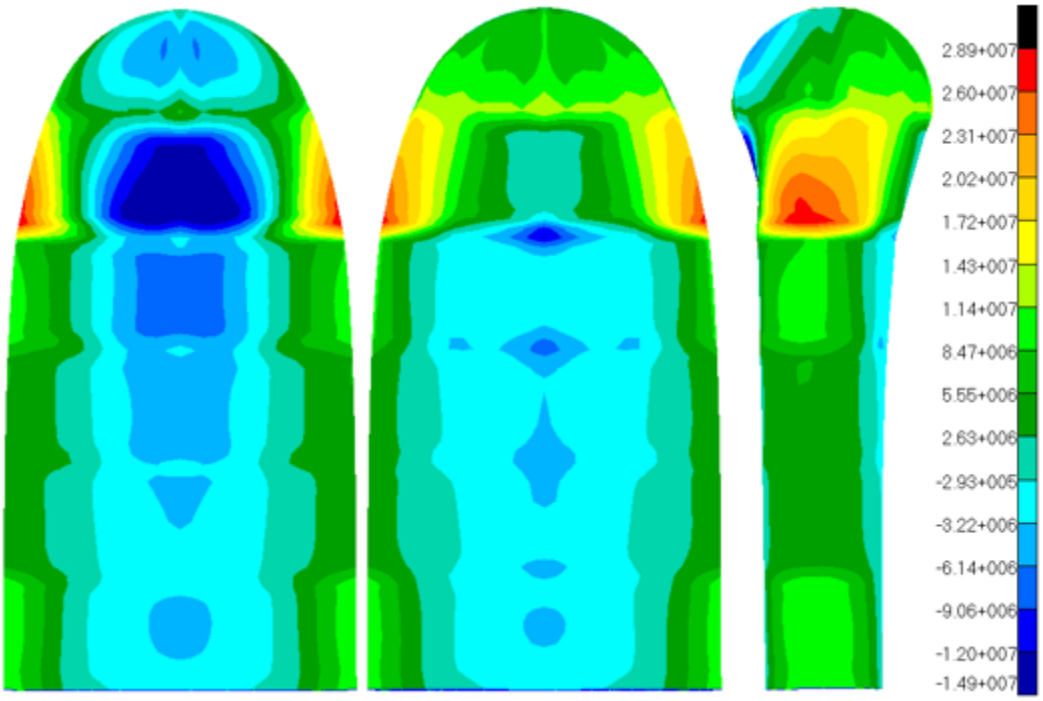

Figure 21: Mars Entry Maximum Principal Stress Contours for Face Sheet (Layer 4)

The allowable stress requirement is 1.5 MPa for the core material and 512 MPa for the face sheet material, and the results in the image show maximum values of 0.381 MPa for the core and 28.9 MPa for the face sheet which means that the highest values for maximum principal stress fall within the reasonable range for the structure.

4.2.2 Buckling

The second analysis that is performed for the Mars entry case is for buckling. While it is not expected that the model will buckle in this phase of the mission nor is the model set up in such a way that it is likely to buckle, the analysis is done for the sake of completeness and to explicitly verify that the buckling requirements for the Mars entry case are met. After running the analysis, the results are given by the F06 file which are shown in Table 10.

Table 10: Mars Entry Buckling Results

		REAL EIGENVALUES				
MODE NO.	EXTRACTION ORDER	EIGENVALUE	RADIANS	CYCLES	GENERALIZED MASS	GENERALIZED STIFFNESS
1	1	2.945909E+00	1.716365E+00	2.731680E-01	1.708531E+05	5.033177E+05
2	2	2.985643E+00	1.727901E+00	2.750040E-01	2.424167E+05	7.237698E+05
3	3	4.399189E+00	2.097424E+00	3.338155E-01	2.217623E+05	9.755745E+05
4	4	4.488459E+00	2.118598E+00	3.371854E-01	2.350269E+05	1.054908E+06
5	5	5.230003E+00	2.286920E+00	3.639746E-01	1.963660E+05	1.026995E+06
6	6	5.296633E+00	2.301441E+00	3.662858E-01	1.588111E+05	8.411642E+05
7	7	6.262737E+00	2.502546E+00	3.982926E-01	2.323404E+05	1.455087E+06
8	8	6.392355E+00	2.528311E+00	4.023931E-01	1.889702E+05	1.207965E+06
9	9	7.156841E+00	2.675227E+00	4.257756E-01	2.080916E+05	1.489278E+06
10	10	7.225679E+00	2.688062E+00	4.278184E-01	1.923782E+05	1.390063E+06

In order for there to be no buckling with the given model and load conditions, all of the eigenvalues must be equal to or greater than one. From the Eigenvalue column in Table 10, it is apparent that all of the values are indeed above one and thus there are no buckling issues for the Mars entry case. In addition, Figure 22 displays the mode shape for the minimum eigenvalue from the buckling analysis which shows the region of deformation close to the top of the structure.

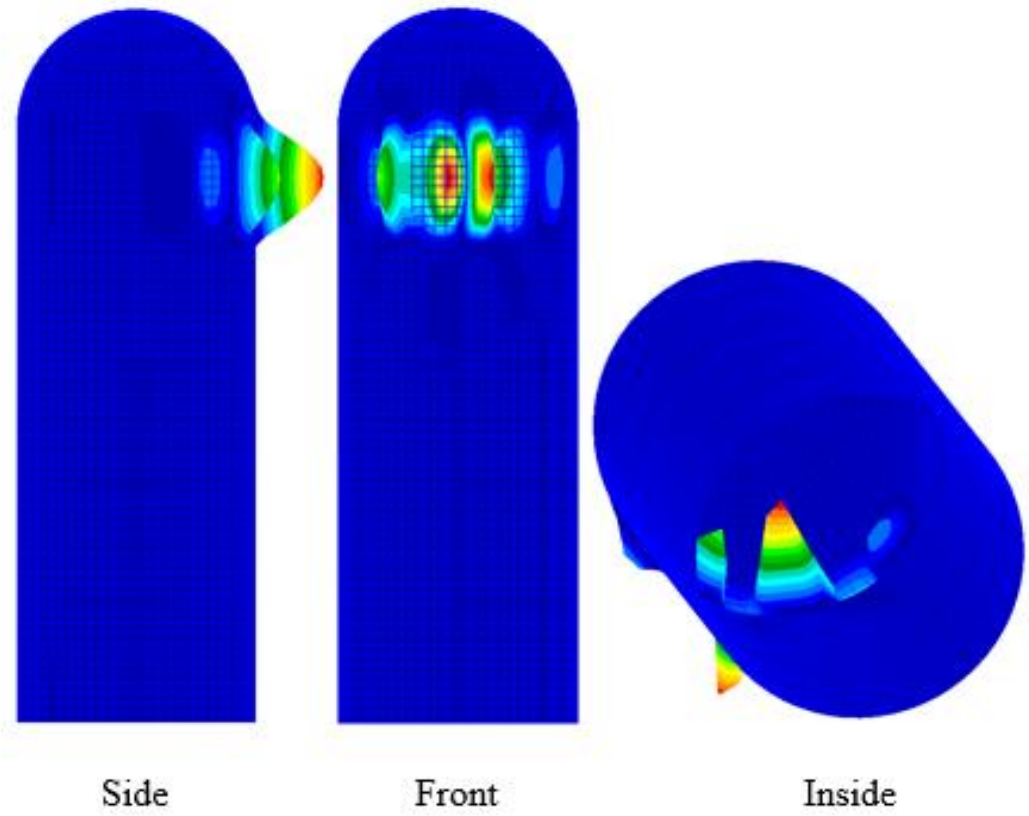

Figure 22. Mars Entry Buckling Contour Mode 1

4.2.3 Normal Modes

The third and last analysis that is performed for the Mars entry case is for normal modes. Just as with buckling, it is not expected that the model will experience any unforced vibrations because it is believed that the frequencies during entry into the Mars atmosphere will be at higher values compared to the natural mode numbers of the structure. However, the results are still shown here to give insight into the modal characteristics of the structure for this load case. For the numerical results of this analysis, the first six mode numbers will have values either at or very close to 0 Hertz. These first six values are known as rigid-body modes and are expected to be at or close to this value. Thus, the lowest mode that must be checked is mode seven. Table 11 shows the output results where mode seven has the lowest value of 4.84 Hertz and the next lowest mode value is 10.57 Hertz.

Table 11: Mars Entry Normal Modes Results

		R E A L E I G E N V A L U E S				
MODE NO.	EXTRACTION ORDER	EIGENVALUE	RADIANS	CYCLES	GENERALIZED MASS	GENERALIZED STIFFNESS
Rigid 1	1	-7.393766E-10	2.719148E-05	4.327658E-06	1.000000E+00	-7.393766E-10
Rigid 2	2	-2.813252E-10	1.677275E-05	2.669466E-06	1.000000E+00	-2.813252E-10
Rigid 3	3	-7.998935E-12	2.828239E-06	4.501282E-07	1.000000E+00	-7.998935E-12
Rigid 4	4	7.994316E-11	8.941094E-06	1.423019E-06	1.000000E+00	7.994316E-11
Rigid 5	5	9.887042E-10	3.144367E-05	5.004415E-06	1.000000E+00	9.887042E-10
Rigid 6	6	1.381760E-09	3.717204E-05	5.916114E-06	1.000000E+00	1.381760E-09
7	7	9.241267E+02	3.039945E+01	4.838223E+00	1.000000E+00	9.241267E+02
8	8	9.241267E+02	3.039945E+01	4.838223E+00	1.000000E+00	9.241267E+02
9	9	4.410768E+03	6.641362E+01	1.057006E+01	1.000000E+00	4.410768E+03
10	10	4.410768E+03	6.641362E+01	1.057006E+01	1.000000E+00	4.410768E+03

While the lowest frequency value for mode seven does not actually meet the requirement for a minimum value of 7 Hertz, it is not expected that there will be any frequency that low during the structure's entry into the Mars atmosphere, so this value should not present any issues. Figure 23 presents two plots where the first one is the deformation pattern for the lowest frequency of 4.84 Hertz and the second plot is the deformation pattern for the second-lowest frequency of 10.57 Hertz. The finite element mesh is shown on top of the deformed contour plots to provide a better picture as to how the original shape has changed. Note that these results are only accurate for the model of the shroud without the internal structure. If the model were to include the internal components, then it would most likely result in an increase in the stiffness which would in turn alter these results.

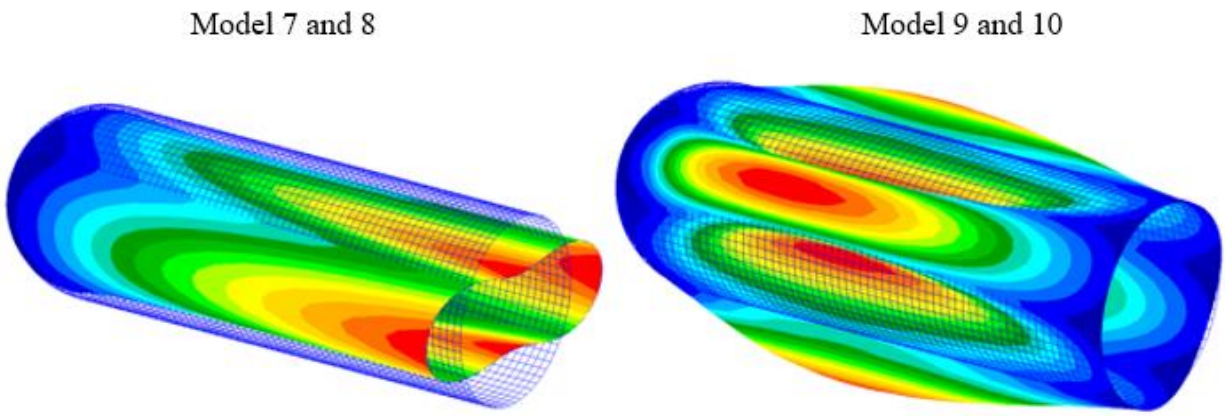

Figure 23. Mars Entry Normal Modes Contours

4.3 Earth Launch Case

4.3.1 Statics

It has already been determined that the Earth launch load case is the driving factor for this model, and the results that are shown in this section are more important in terms of remaining within all acceptable limits. In addition to the statics, buckling, and normal modes results, the Earth launch load case also consists of the vibro-acoustics analysis which determines if the vibrations from the initial stage of launch will have any adverse effect on the structure.

The first set of results which are shown in Figure 24 are the deformation results for the static analysis which are exaggerated to make it easier to see them. Also, as with the figures in the last section, the label “front” refers to the side that is facing the windward direction, the label “back” indicates the leeward side, and the label “side” refers to the view that is perpendicular to the windward direction.

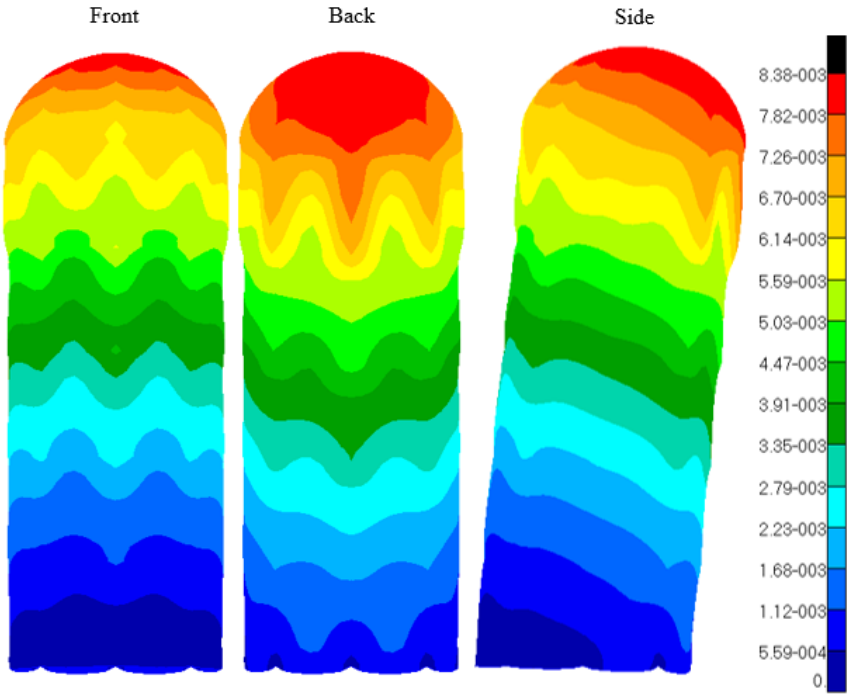

Figure 24. Earth Launch Deformation Contour

This image shows that the structure keeps its shape and the bottom stays stationary while the top end tilts backwards, though only by a few millimeters; these are acceptable results for the physical deformation. However, the bottom does show major local deformation at the longeron connection points. In order to relieve some stress from those points and increase the stiffness, a payload adaptor can potentially be used to distribute some of the load to the thirty six plies that the shell has at the bottom of the structure. The next plot is in Figure 25 which displays the contours for the maximum bar stresses which is the superposition of the axial and bending bar stresses.

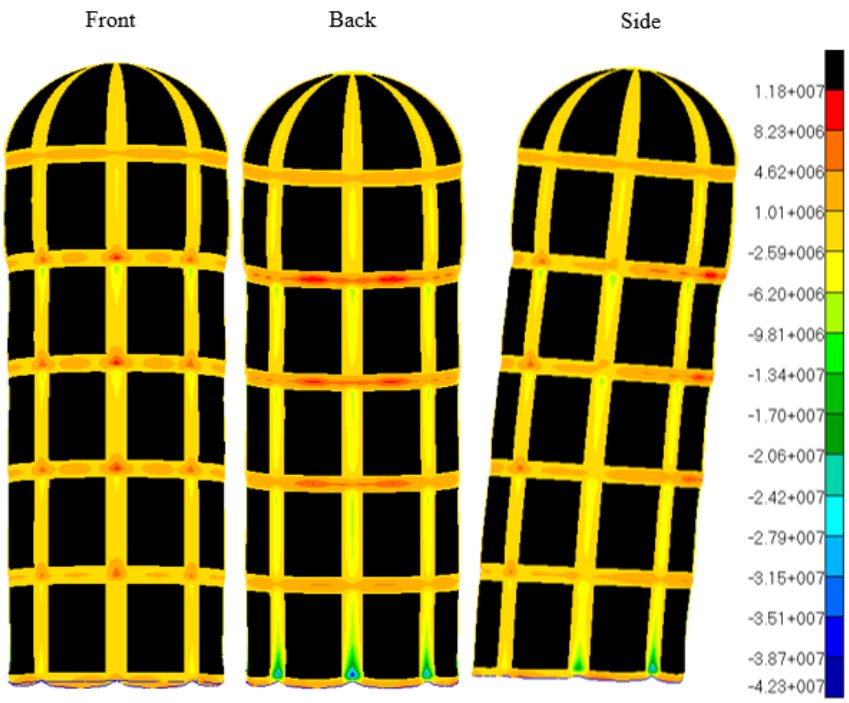

Figure 25. Earth Launch Bar Stress Contour

As seen again from the table in the Materials section, the allowable stress requirement is 512 MPa whereas the results in the image show a maximum value of 11.8 MPa, so the bar stress values are within the acceptable range for this load case as well. Next are the plots for maximum principal stress. There are four layers of the composite shell which are the two face sheets and the honeycomb core split into equal halves, but only the two plots with the higher values will be shown. Just as with the pervious case, the inner honeycomb core and the inner face sheet sections have the higher maximum principal stress which are shown in Figure 26 and Figure 27, respectively.

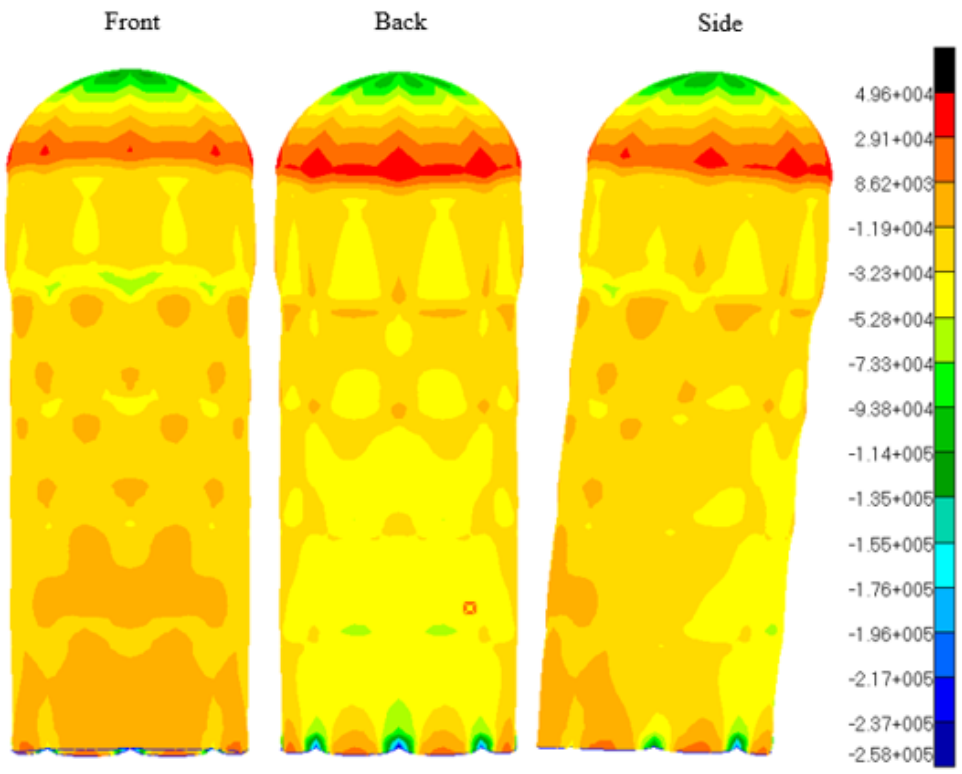

Figure 26. Earth Launch Maximum Principal Stress Contours for Honeycomb Core (Layer 3)

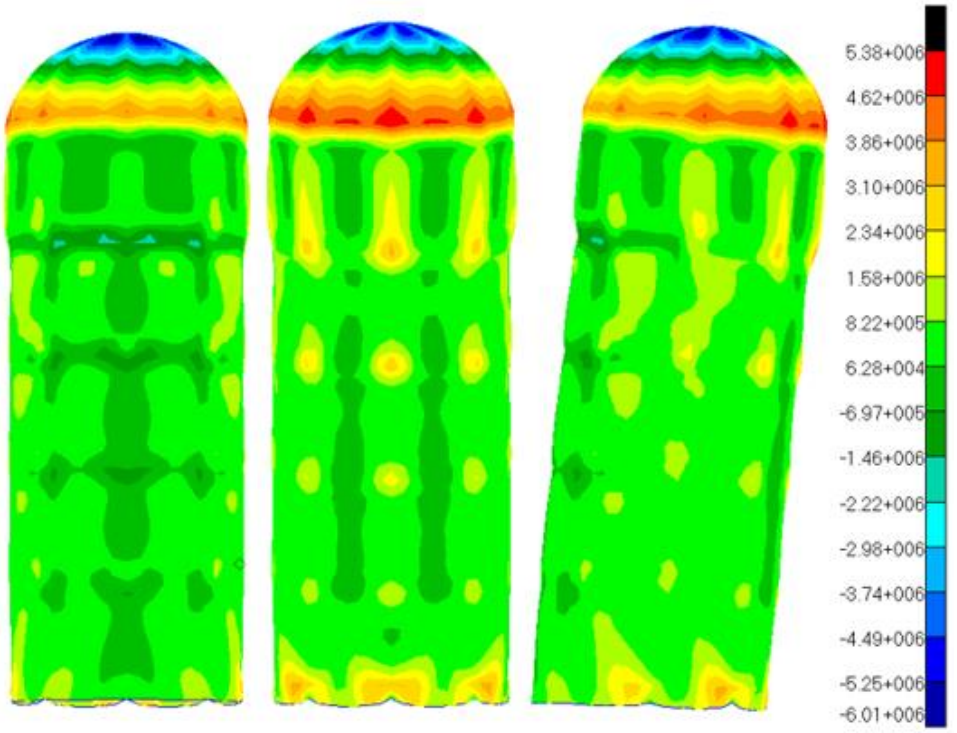

Figure 27: Earth Launch Maximum Principal Stress Contours for Face Sheet (Layer 4)

Once again, the allowable stress requirement is 1.5 MPa for the core material and 512 MPa for the face sheet material, and the results in the image show maximum values of 0.0496 MPa for the core and 5.38 MPa for the face sheet which means that the highest values for maximum principal stress fall within the reasonable range for the structure.

4.3.2 Buckling

The second analysis is buckling, and unlike the Mars entry load case, the Earth launch load case is set up such that buckling is expected to occur if the model dimensions and parameter values are not assigned proper values to prevent it. Thus, it is important that the results indicate that no buckling occurs during launch. After running the analysis, the results are given by the F06 file which are shown in Table 12.

Table 12: Earth Launch Buckling Results

R E A L E I G E N V A L U E S

MODE NO.	EXTRACTION ORDER	EIGENVALUE	RADIANS	CYCLES	GENERALIZED MASS	GENERALIZED STIFFNESS
1	1	2.355887E+01	4.853748E+00	7.724980E-01	3.230432E+06	7.610533E+07
2	2	2.727356E+01	5.222409E+00	8.311722E-01	1.122134E+07	3.060458E+08
3	3	2.728231E+01	5.223247E+00	8.313056E-01	1.115277E+07	3.042733E+08
4	4	3.717193E+01	6.096879E+00	9.703484E-01	2.461860E+06	9.151210E+07
5	5	3.792508E+01	6.158334E+00	9.801293E-01	8.582651E+04	3.254977E+06
6	6	3.796570E+01	6.161632E+00	9.806541E-01	8.617092E+04	3.271540E+06
7	7	3.807476E+01	6.170475E+00	9.820616E-01	6.675110E+04	2.541532E+06
8	8	3.807505E+01	6.170498E+00	9.820653E-01	7.438178E+04	2.832090E+06
9	9	3.833303E+01	6.191368E+00	9.853868E-01	1.424279E+05	5.459692E+06
10	10	3.835067E+01	6.192792E+00	9.856134E-01	1.468917E+05	5.633395E+06

In order for there to be no buckling with the given model and load conditions, all of the eigenvalues must be equal to or greater than one. From the Eigenvalue column in the figure, it can be seen that all of the values are indeed above one and thus there are no buckling issues for the Earth launch case. In addition, Figure 28 displays the plots of the deformation from the buckling analysis.

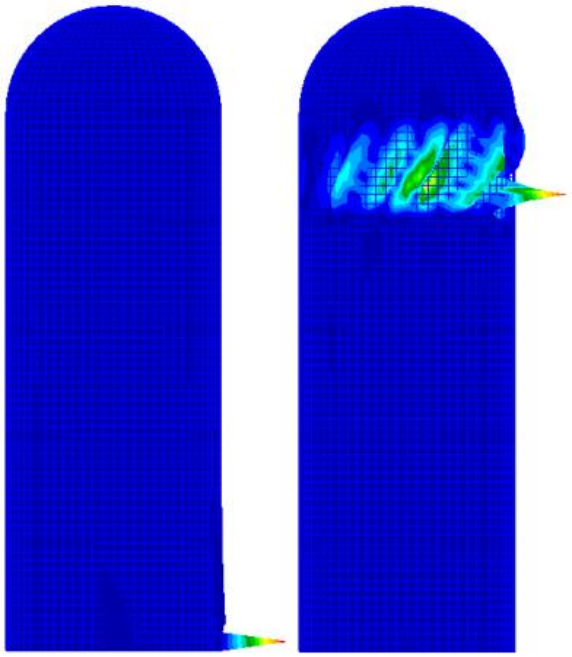

Figure 28. Earth Launch Buckling Contours Modes 1 (left) & 5 (right)

4.3.3 Normal Modes

The third analysis is the modal analysis, and with the launch of the structure off of Earth the natural vibrations can have a large effect if they are not accounted for properly in the design optimization. After running the design optimization, the contour plot can be generated and is shown in Figure 29. Also, Figure 30 shows the normal mode values from the F06 file, and from the Cycles column it can be seen that the lowest mode number nearly meets the requirement of a minimum value of 7 Hertz.

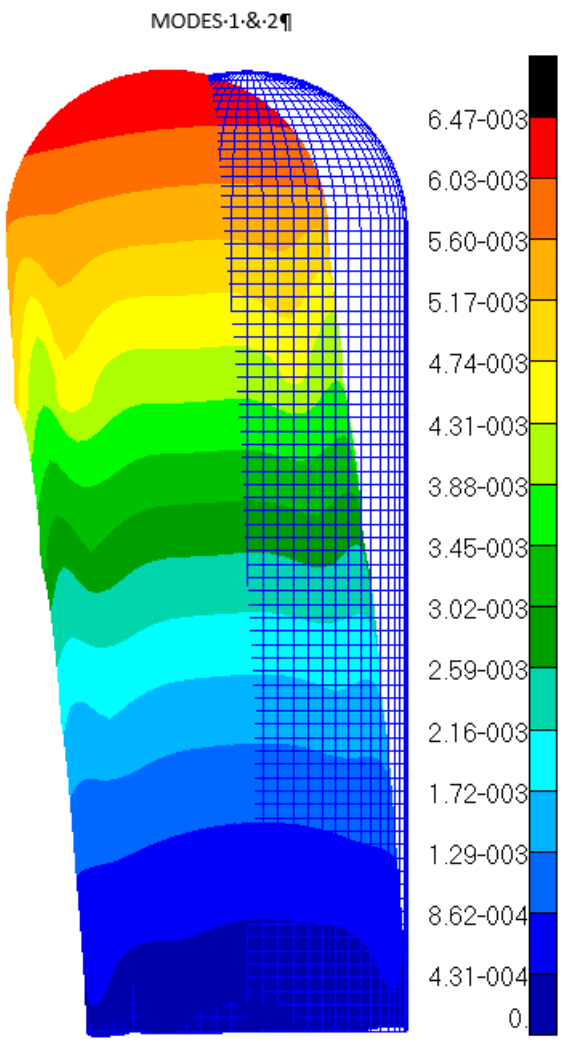

Figure 29. Earth Launch Normal Modes Contour

R E A L E I G E N V A L U E S
(BEFORE AUGMENTATION OF RESIDUAL VECTORS)

MODE NO.	EXTRACTION ORDER	EIGENVALUE	RADIANS	CYCLES	GENERALIZED MASS	GENERALIZED STIFFNESS
1	1	1.924766E+03	4.387216E+01	6.982471E+00	1.000000E+00	1.924766E+03
2	2	1.924766E+03	4.387216E+01	6.982471E+00	1.000000E+00	1.924766E+03
3	3	5.163802E+03	7.185960E+01	1.143681E+01	1.000000E+00	5.163802E+03
4	4	5.163802E+03	7.185960E+01	1.143681E+01	1.000000E+00	5.163802E+03
5	5	5.778389E+03	7.601572E+01	1.209828E+01	1.000000E+00	5.778389E+03
6	6	5.778389E+03	7.601572E+01	1.209828E+01	1.000000E+00	5.778389E+03
7	7	1.244237E+04	1.115454E+02	1.775300E+01	1.000000E+00	1.244237E+04
8	8	1.249880E+04	1.117980E+02	1.779321E+01	1.000000E+00	1.249880E+04
9	9	1.308648E+04	1.143962E+02	1.820672E+01	1.000000E+00	1.308648E+04
10	10	1.308648E+04	1.143962E+02	1.820672E+01	1.000000E+00	1.308648E+04

Figure 30. Earth Launch Normal Modes Results

4.3.4 Vibro-acoustics

Unlike the Mars entry case, the Earth launch case has one other load case which is the vibrations caused by the acoustic noise generated by the initial stage of the launch. The input file information for this part of the analysis is displayed in Appendices A.2 and B.2. After running the analysis in Nastran, the composite-based set of results, shown in Appendix C, from the F06 file with the minimum, maximum, and RMS values in the upper table and the graph displayed below it. To start with, by reading YMIN and YMAX values from the table, it seems to be that the vibration caused by the acoustics from the launch has no effect on the structure. However, to be absolutely sure that there is no effect, the RMS value, which is the square root of the area under the curve, must be multiplied by a scalar value of three to get the equivalent peak value and compared to the allowable stress value. Looking at the figure shows an RMS value of 17.8 Pa, and this value multiplied by a scalar value of three is 53.4 Pa. The lowest value of the allowable stress is 1.48 MPa, so the vibrations from launch will not have any substantial effect on the structure which means that there should be no issues from the continuation of the project without consideration of the launch vibrations.

5 Conclusion and Recommendations

5.1 Final Outcome

In terms of the work done and documented for the finite element analysis of the Rigid Mid-Range Lift to Drag Ratio Aeroshell, the project is a success with a significant amount of progress and improvements made compared to the past model and analyses performed. The setup of the loads and boundary conditions is refined with more accurate representation of the condition that would be encountered by the structure. The most noteworthy improvement of the model is the use of the inertia relief to model the fact that there will be no constraints on the model during entry into the Mars atmosphere. In addition, the values assigned to the loads are more accurate, particularly with the gravity loads which had not been representative of the launch vehicle that will most likely carry this structure into space. The implementation of the design optimization should also make it easier to significantly reduce the mass of the aeroshell and still keep it fully functional. Not only has the finite element analysis been successful, but the development of the Python code that is used to generate the model and submit the analysis runs has made the process more convenient (Lane 2017).

One of the important outcomes of the effort put into this work was the conclusion that the Earth launch case is the driver of the optimization and analysis of the model. It will define how the structure is made, though the resulting model should still be analyzed under the Mars entry conditions to make sure that it works in that case as well. In addition to that, one important lesson is that the mass estimates from previously developed models were significantly

underestimated, and as a results it is possible that the design of the aeroshell might need to be altered or even completely redone. This underestimation might have been caused by the previous model not being analyzed for all three of the subcases from the design optimization. Also, the payload needed to be completely remodeled in the baseline, by changing from one mass element with one-hundred twenty-eight RBE3 links to four mass elements each with eight links and all attached to each other with rod elements. Lastly, design and requirements were changed during the development of the finite element model which needed to be incorporated into an updated model.

5.2 Recommendations for further study

Even with the major success and developments made with this work, there is still much more that needs to be done. First, one simple yet necessary change to make is to the loads for the rocket that will actually be used to launch the structure. Most of the data used were for a Delta IV Heavy rocket which is not big enough to take the aeroshell into space. The data that needs to be changed are the gravity loads and the table of vibration values for the vibro-acoustic analysis, and it is possible that the pressure load might need to be changed as well. Also, it must be specified at which stages of launch these values are associated.

Another area where improvements must be made is in the design optimization. One update that can be made is to the longeron beam elements. In the design optimization, all of the longerons were grouped together and each longeron individually was not split into parts for multiple groups. In order to get a more refined result for the design optimization, all of the longerons bars should be in separate groups and each individual longeron should be separated exactly like the shell sections where each partial piece should be in its own group. In other words, the optimization for the updated longerons will behave similar to the shell sections.

Another improvement is to determine a reliable method to pick the initial values for the design variables. Most of the work to overcome obstacles and issues with the design optimization involved trying to determine the best initial values to select. Not only can the choice of the initial values result in higher optimized mass values, but they have also produced issues with the large beam cross-section dimensions being assigned values lower than the low cross-section dimensions which produced a fatal error during the analysis. Unfortunately, it has been determined that there is no solid method to use for picking the initial values, though a reliable approach for this model would increase the convenience of the parametric study.

The design optimization results indicated that there may need to be changes made to the design of the finite element model, and if this ends up being the case then one of the best improvement that can be made is to the setup of the beam elements. The beams already on the model can be kept, but in order to better prevent issues such as buckling and modal vibration, it is possible to add more elements such as batons. These are essentially beam elements that diagonally twist around and down the structure in a screw fashion. While it is not guaranteed that this will help, it is definitely worth some consideration.

One more improvement to make that was mentioned in the previous section is to keep redesigning the model of the payload and its attachments. To be more specific, the redistribution of the mass element should be fine, but the number of RBE3 links needs to be reduced. At most, there should be three to five RBE3 links as opposed to the current 32 for the baseline model.

Finally, there is another load condition that must be added to the model which is a thermal loads case. This is needed to represent the extreme heat that the model will be exposed to during its entry into the Mars atmosphere. This is an important load to incorporate since extreme heat can have a serious effect on a structure and, if not accounted for, can cause the structure to fail in its descent towards the surface of Mars.

References

Dwyer-Cianciolo, A. M., et al., "Entry, Descent and Landing Systems Analysis Study: Phase 1 Report," NASA TM-216720, 2010.

HyperSizer Structural Sizing Software. Collier Research Corporation, 1998.

Lane, B. M., Ahmed, S. W., "Parametric Structural Model for a Mars Entry Concept," NASA TM-219375, 2017.

MD Nastran 2006 r1 Quick Reference Guide (Vols. 1-3). MSC.Software Corporation, 2006.

Moore, G. J. *MSC/Nastran Design Sensitivity and Optimization User's Guide, Version 67,* The MacNeal-Schwendler Corporation, 1994.

Walker, S. P., Daryabeigi, K., Samareh, J. A., Armand, S. C., "Preliminary Development of a Multifunctional Hot Structure Heat Shield," AIAA 2014-0350, 2014.

Appendix A: BDF Case Control Sections for Case #1

A.1: Statics (SOL 101)

```
$==========Case:1==========$
$ Mars Reentry Vehicle
$ Diameter:10
$ Length:30
$ Element Sizing:60
$ Number of Elements per Ring:64$
nastran system(107)=4
SOL 101
CEND
ECHO = NONE
SUBCASE 101
$ Subcase name: Entry
    SUBTITLE = Entry
    LOAD = 3
    DISPLACEMENT(SORT1,REAL)=ALL
    SPCFORCES(SORT1,REAL)=ALL
    MPCFORCES(SORT1,REAL)=ALL
    STRESS(SORT1,REAL,VONMISES,BILIN)=ALL
    FORCE(SORT1,REAL,BILIN)=ALL
    PARAM,INREL,-2
SUBCASE 151
$ Subcase name:Launch_1
    SUBTITLE = Launch_1
    SPC = 7
    LOAD = 6
    DISPLACEMENT(SORT1,REAL)=ALL
    SPCFORCES(SORT1,REAL)=ALL
    MPCFORCES(SORT1,REAL)=ALL
    STRESS(SORT1,REAL,VONMISES,BILIN)=ALL
    FORCE(SORT1,REAL,BILIN)=ALL
$
```

A.2: Frequency Response (SOL 111)

```
$==========Case:1==========$
$ Mars Reentry Vehicle - Vibro-acoustic Analysis$
nastran system(107)=4$
SOL 111
CEND
ECHO = NONE
RESVEC = NO
SDAMPING(STRUCTURE) = 2
METHOD(STRUCTURE) = 9
STRESS(PLOT) = ALL
RANDOM = 13
FREQUENCY = 8
```

```
SPC = 7
SUBCASE 1
$ Subcase name: Vibro_Acoustics_during_lauch_1
    SUBTITLE = Vibro-Acoustics during initial lauch_1
    DLOAD = 12
OUTPUT(XYPLOT)
YBLOG(YES)
YLOG=YES
YAXIS=YES
XLOG=YES
YAXIS=YES
XTITLE=FREQUENCY (Hz)
YTITLE=X-DIR PSDF OF ELEMENT STRESS (Pa)^2/Hz 68 LAYER 1
XYPEAK,XYPRINT,XYPLOT,XYPAPLOT,CSIG,PSDF / 68(-1,9)
YTITLE=X-DIR PSDF OF ELEMENT STRESS (Pa)^2/Hz 68 LAYER 2
XYPEAK,XYPRINT,XYPLOT,XYPAPLOT,CSIG,PSDF / 68(-2,9)
YTITLE=X-DIR PSDF OF ELEMENT STRESS (Pa)^2/Hz 68 LAYER 3
XYPEAK,XYPRINT,XYPLOT,XYPAPLOT,CSIG,PSDF / 68(-3,9)
YTITLE=X-DIR PSDF OF ELEMENT STRESS (Pa)^2/Hz 68 LAYER 4
XYPEAK,XYPRINT,XYPLOT,XYPAPLOT,CSIG,PSDF / 68(-4,9)
$
```

A.3: Design Optimization (SOL 200)

```
$==========Case:1==========$
$ Mars Reentry Vehicle - Design Optimization$
nastran system(107)=4$
SOL 200
CEND
ECHO = NONE
DESOBJ(MIN) = 1
ELSUM(PIDSUM)=ALL
SUBCASE 1
$ Subcase name: Design Optimization 1
    SUBTITLE = Design_Optimization_1
    ANALYSIS = STATICS
    SPC = 7
    LOAD = 6
    DISPLACEMENT(SORT1,REAL,plot)=ALL
    SPCFORCES(SORT1,REAL,plot)=ALL
    STRESS(SORT1,REAL,VONMISES,BILIN,plot)=ALL
    DESSUB = 1
$
```

Appendix B: BDF Bulk Data Sections for Case #1

B.1: Statics (SOL 101)

Nodes

EXAMPLE SET OF NODES IN HEMISPHERE

```
GRID,1, ,-5.0,0.0,0.0
GRID,2, ,-4.8939168279,1.02448918079,0.0
GRID,3, ,-4.8939168279,1.01955598537,0.1004174998
GRID,4, ,-4.8939168279,1.00480390846,0.199867924183
GRID,5, ,-4.8939168279,0.980375020623,0.297393511197
GRID,6, ,-4.8939168279,0.946504585415,0.392055036127
GRID,7, ,-4.8939168279,0.903518793637,0.48294085674
GRID,8, ,-4.8939168279,0.851831621963,0.5691756929
GRID,9, ,-4.8939168279,0.791940846111,0.649929055994
GRID,10, ,-4.8939168279,0.724423246992,0.724423246992
GRID,11, ,-4.8939168279,0.649929055994,0.791940846111
GRID,12, ,-4.8939168279,0.5691756929,0.851831621963
GRID,13, ,-4.8939168279,0.48294085674,0.903518793637
GRID,14, ,-4.8939168279,0.392055036127,0.946504585415
GRID,15, ,-4.8939168279,0.297393511197,0.980375020623
GRID,16, ,-4.8939168279,0.199867924183,1.00480390846
GRID,17, ,-4.8939168279,0.1004174998,1.01955598537
GRID,18, ,-4.8939168279,6.2731869801e-17,1.02448918079
GRID,19, ,-4.8939168279,-0.1004174998,1.01955598537
GRID,20, ,-4.8939168279,-0.199867924183,1.00480390846
GRID,21, ,-4.8939168279,-0.297393511197,0.980375020623
GRID,22, ,-4.8939168279,-0.392055036127,0.946504585415
GRID,23, ,-4.8939168279,-0.48294085674,0.903518793637
GRID,24, ,-4.8939168279,-0.5691756929,0.851831621963
GRID,25, ,-4.8939168279,-0.649929055994,0.791940846111
GRID,26, ,-4.8939168279,-0.724423246992,0.724423246992
GRID,27, ,-4.8939168279,-0.791940846111,0.649929055994
GRID,28, ,-4.8939168279,-0.851831621963,0.5691756929
GRID,29, ,-4.8939168279,-0.903518793637,0.48294085674
GRID,30, ,-4.8939168279,-0.946504585415,0.392055036127
GRID,31, ,-4.8939168279,-0.980375020623,0.297393511197
GRID,32, ,-4.8939168279,-1.00480390846,0.199867924183
GRID,33, ,-4.8939168279,-1.01955598537,0.1004174998
GRID,34, ,-4.8939168279,-1.02448918079,1.25463739602e-16
GRID,35, ,-4.8939168279,-1.01955598537,-0.1004174998
GRID,36, ,-4.8939168279,-1.00480390846,-0.199867924183
GRID,37, ,-4.8939168279,-0.980375020623,-0.297393511197
GRID,38, ,-4.8939168279,-0.946504585415,-0.392055036127
GRID,39, ,-4.8939168279,-0.903518793637,-0.48294085674
GRID,40, ,-4.8939168279,-0.851831621963,-0.5691756929
GRID,41, ,-4.8939168279,-0.791940846111,-0.649929055994
GRID,42, ,-4.8939168279,-0.724423246992,-0.724423246992
GRID,43, ,-4.8939168279,-0.649929055994,-0.791940846111
```

```
GRID,44, ,-4.8939168279,-0.5691756929,-0.851831621963
GRID,45, ,-4.8939168279,-0.48294085674,-0.903518793637
GRID,46, ,-4.8939168279,-0.392055036127,-0.946504585415
GRID,47, ,-4.8939168279,-0.297393511197,-0.980375020623
GRID,48, ,-4.8939168279,-0.199867924183,-1.00480390846
GRID,49, ,-4.8939168279,-0.1004174998,-1.01955598537
GRID,50, ,-4.8939168279,-1.88195609403e-16,-1.02448918079
GRID,51, ,-4.8939168279,0.1004174998,-1.01955598537
GRID,52, ,-4.8939168279,0.199867924183,-1.00480390846
GRID,53, ,-4.8939168279,0.297393511197,-0.980375020623
GRID,54, ,-4.8939168279,0.392055036127,-0.946504585415
GRID,55, ,-4.8939168279,0.48294085674,-0.903518793637
GRID,56, ,-4.8939168279,0.5691756929,-0.851831621963
GRID,57, ,-4.8939168279,0.649929055994,-0.791940846111
GRID,58, ,-4.8939168279,0.724423246992,-0.724423246992
GRID,59, ,-4.8939168279,0.791940846111,-0.649929055994
GRID,60, ,-4.8939168279,0.851831621963,-0.5691756929
GRID,61, ,-4.8939168279,0.903518793637,-0.48294085674
GRID,62, ,-4.8939168279,0.946504585415,-0.392055036127
GRID,63, ,-4.8939168279,0.980375020623,-0.297393511197
GRID,64, ,-4.8939168279,1.00480390846,-0.199867924183
GRID,65, ,-4.8939168279,1.01955598537,-0.1004174998
```


EXAMPLE SET OF NODES IN CYLINDER

```
GRID,3074, ,12.5,5.0,0.0
GRID,3075, ,12.5,4.97592363336,0.490085701648
GRID,3076, ,12.5,4.90392640202,0.975451610081
GRID,3077, ,12.5,4.78470167866,1.45142338627
GRID,3078, ,12.5,4.61939766256,1.91341716183
GRID,3079, ,12.5,4.40960632174,2.35698368413
GRID,3080, ,12.5,4.15734806151,2.7778511651
GRID,3081, ,12.5,3.86505226681,3.17196642082
GRID,3082, ,12.5,3.53553390593,3.53553390593
GRID,3083, ,12.5,3.17196642082,3.86505226681
GRID,3084, ,12.5,2.7778511651,4.15734806151
GRID,3085, ,12.5,2.35698368413,4.40960632174
GRID,3086, ,12.5,1.91341716183,4.61939766256
GRID,3087, ,12.5,1.45142338627,4.78470167866
GRID,3088, ,12.5,0.975451610081,4.90392640202
GRID,3089, ,12.5,0.490085701648,4.97592363336
GRID,3090, ,12.5,3.06161699787e-16,5.0
GRID,3091, ,12.5,-0.490085701648,4.97592363336
GRID,3092, ,12.5,-0.975451610081,4.90392640202
GRID,3093, ,12.5,-1.45142338627,4.78470167866
GRID,3094, ,12.5,-1.91341716183,4.61939766256
GRID,3095, ,12.5,-2.35698368413,4.40960632174
GRID,3096, ,12.5,-2.7778511651,4.15734806151
GRID,3097, ,12.5,-3.17196642082,3.86505226681
GRID,3098, ,12.5,-3.53553390593,3.53553390593
GRID,3099, ,12.5,-3.86505226681,3.17196642082
GRID,3100, ,12.5,-4.15734806151,2.7778511651
```

```
GRID,3101, ,12.5,-4.40960632174,2.35698368413
GRID,3102, ,12.5,-4.61939766256,1.91341716183
GRID,3103, ,12.5,-4.78470167866,1.45142338627
GRID,3104, ,12.5,-4.90392640202,0.975451610081
GRID,3105, ,12.5,-4.97592363336,0.490085701648
GRID,3106, ,12.5,-5.0,6.12323399574e-16
GRID,3107, ,12.5,-4.97592363336,-0.490085701648
GRID,3108, ,12.5,-4.90392640202,-0.975451610081
GRID,3109, ,12.5,-4.78470167866,-1.45142338627
GRID,3110, ,12.5,-4.61939766256,-1.91341716183
GRID,3111, ,12.5,-4.40960632174,-2.35698368413
GRID,3112, ,12.5,-4.15734806151,-2.7778511651
GRID,3113, ,12.5,-3.86505226681,-3.17196642082
GRID,3114, ,12.5,-3.53553390593,-3.53553390593
GRID,3115, ,12.5,-3.17196642082,-3.86505226681
GRID,3116, ,12.5,-2.7778511651,-4.15734806151
GRID,3117, ,12.5,-2.35698368413,-4.40960632174
GRID,3118, ,12.5,-1.91341716183,-4.61939766256
GRID,3119, ,12.5,-1.45142338627,-4.78470167866
GRID,3120, ,12.5,-0.975451610081,-4.90392640202
GRID,3121, ,12.5,-0.490085701648,-4.97592363336
GRID,3122, ,12.5,-9.18485099361e-16,-5.0
GRID,3123, ,12.5,0.490085701648,-4.97592363336
GRID,3124, ,12.5,0.975451610081,-4.90392640202
GRID,3125, ,12.5,1.45142338627,-4.78470167866
GRID,3126, ,12.5,1.91341716183,-4.61939766256
GRID,3127, ,12.5,2.35698368413,-4.40960632174
GRID,3128, ,12.5,2.7778511651,-4.15734806151
GRID,3129, ,12.5,3.17196642082,-3.86505226681
GRID,3130, ,12.5,3.53553390593,-3.53553390593
GRID,3131, ,12.5,3.86505226681,-3.17196642082
GRID,3132, ,12.5,4.15734806151,-2.7778511651
GRID,3133, ,12.5,4.40960632174,-2.35698368413
GRID,3134, ,12.5,4.61939766256,-1.91341716183
GRID,3135, ,12.5,4.78470167866,-1.45142338627
GRID,3136, ,12.5,4.90392640202,-0.975451610081
GRID,3137, ,12.5,4.97592363336,-0.490085701648
```


REFERENCE NODES IN CENTER OF CYLINDER

```
GRID,5058, ,0.0,0.0,0.0
GRID,5059, ,0.416666666667,0.0,0.0
GRID,5060, ,0.833333333333,0.0,0.0
GRID,5061, ,1.25,0.0,0.0
GRID,5062, ,1.66666666667,0.0,0.0
GRID,5063, ,2.08333333333,0.0,0.0
GRID,5064, ,2.5,0.0,0.0
GRID,5065, ,2.91666666667,0.0,0.0
GRID,5066, ,3.33333333333,0.0,0.0
GRID,5067, ,3.75,0.0,0.0
GRID,5068, ,4.16666666667,0.0,0.0
GRID,5069, ,4.58333333333,0.0,0.0
```

```
GRID,5070, ,5.0,0.0,0.0
GRID,5071, ,5.41666666667,0.0,0.0
GRID,5072, ,5.83333333333,0.0,0.0
GRID,5073, ,6.25,0.0,0.0
GRID,5074, ,6.66666666667,0.0,0.0
GRID,5075, ,7.08333333333,0.0,0.0
GRID,5076, ,7.5,0.0,0.0
GRID,5077, ,7.91666666667,0.0,0.0
GRID,5078, ,8.33333333333,0.0,0.0
GRID,5079, ,8.75,0.0,0.0
GRID,5080, ,9.16666666667,0.0,0.0
GRID,5081, ,9.58333333333,0.0,0.0
GRID,5082, ,10.0,0.0,0.0
GRID,5083, ,10.4166666667,0.0,0.0
GRID,5084, ,10.8333333333,0.0,0.0
GRID,5085, ,11.25,0.0,0.0
GRID,5086, ,11.6666666667,0.0,0.0
GRID,5087, ,12.0833333333,0.0,0.0
GRID,5088, ,12.5,0.0,0.0
GRID,5089, ,12.9166666667,0.0,0.0
GRID,5090, ,13.3333333333,0.0,0.0
GRID,5091, ,13.75,0.0,0.0
GRID,5092, ,14.1666666667,0.0,0.0
GRID,5093, ,14.5833333333,0.0,0.0
GRID,5094, ,15.0,0.0,0.0
GRID,5095, ,15.4166666667,0.0,0.0
GRID,5096, ,15.8333333333,0.0,0.0
GRID,5097, ,16.25,0.0,0.0
GRID,5098, ,16.6666666667,0.0,0.0
GRID,5099, ,17.0833333333,0.0,0.0
GRID,5100, ,17.5,0.0,0.0
GRID,5101, ,17.9166666667,0.0,0.0
GRID,5102, ,18.3333333333,0.0,0.0
GRID,5103, ,18.75,0.0,0.0
GRID,5104, ,19.1666666667,0.0,0.0
GRID,5105, ,19.5833333333,0.0,0.0
GRID,5106, ,20.0,0.0,0.0
GRID,5107, ,20.4166666667,0.0,0.0
GRID,5108, ,20.8333333333,0.0,0.0
GRID,5109, ,21.25,0.0,0.0
GRID,5110, ,21.6666666667,0.0,0.0
GRID,5111, ,22.0833333333,0.0,0.0
GRID,5112, ,22.5,0.0,0.0
GRID,5113, ,22.9166666667,0.0,0.0
GRID,5114, ,23.3333333333,0.0,0.0
GRID,5115, ,23.75,0.0,0.0
GRID,5116, ,24.1666666667,0.0,0.0
GRID,5117, ,24.5833333333,0.0,0.0
GRID,5118, ,25.0,0.0,0.0
```

MATERIALS AND ELEMENT PROPERTIES

```
$========== MATERIALS: ==========$
MAT1,300,5.80E+10,2.21E+10,,1580.0
MAT1,301,5.17E+08,1.52E+08,,49.57387941
MAT1,200,5.80E+10,2.21E+10,,1580.0
MAT1,201,5.80E+10,2.21E+10,,1580.0
MAT1,202,5.80E+10,2.21E+10,,1580.0
MAT1,203,5.80E+10,2.21E+10,,1580.0
MAT1,1000,68300000000.0,,0.3,0.0
$========== PROPERTIES: ==========$
PCOMP,30000,,9.8,279358100.0,,,,SYM
,300,0.02,0.0
,301,0.1,0.0
PCOMP,30001,,9.8,279358100.0,,,,SYM
,300,0.02,0.0
,301,0.1,0.0
PCOMP,30002,,9.8,279358100.0,,,,SYM
,300,0.02,0.0
,301,0.1,0.0
PCOMP,30003,,9.8,279358100.0,,,,SYM
,300,0.02,0.0
,301,0.1,0.0
PCOMP,30004,,9.8,279358100.0,,,,SYM
,300,0.02,0.0
,301,0.1,0.0
PCOMP,30005,,9.8,279358100.0,,,,SYM
,300,0.02,0.0
,301,0.1,0.0
PBARL,20000,200,,CHAN2
,0.04,0.04,0.3,0.3
PBARL,22000,201,,CHAN2
,0.02,0.02,0.15,0.15
PBARL,22001,202,,CHAN2
,0.04,0.04,0.3,0.3
PBARL,22002,203,,CHAN2
,0.04,0.04,0.3,0.3
PROD,10000,1000,0.00258064,1.05992462e-06,0.028660831
```

TRIA ELEMENTS AND EXAMPLE SET OF QUAD ELEMENTS

```
$========== ELEMENTS: ==========$
CTRIA3,1,30000,1,3,2,,
CTRIA3,2,30000,1,4,3,,
CTRIA3,3,30000,1,5,4,,
CTRIA3,4,30000,1,6,5,,
CTRIA3,5,30000,1,7,6,,
CTRIA3,6,30000,1,8,7,,
CTRIA3,7,30000,1,9,8,,
CTRIA3,8,30000,1,10,9,,
CTRIA3,9,30000,1,11,10,,
CTRIA3,10,30000,1,12,11,,
CTRIA3,11,30000,1,13,12,,
```

```
CTRIA3,12,30000,1,14,13,,
CTRIA3,13,30000,1,15,14,,
CTRIA3,14,30000,1,16,15,,
CTRIA3,15,30000,1,17,16,,
CTRIA3,16,30000,1,18,17,,
CTRIA3,17,30000,1,19,18,,
CTRIA3,18,30000,1,20,19,,
CTRIA3,19,30000,1,21,20,,
CTRIA3,20,30000,1,22,21,,
CTRIA3,21,30000,1,23,22,,
CTRIA3,22,30000,1,24,23,,
CTRIA3,23,30000,1,25,24,,
CTRIA3,24,30000,1,26,25,,
CTRIA3,25,30000,1,27,26,,
CTRIA3,26,30000,1,28,27,,
CTRIA3,27,30000,1,29,28,,
CTRIA3,28,30000,1,30,29,,
CTRIA3,29,30000,1,31,30,,
CTRIA3,30,30000,1,32,31,,
CTRIA3,31,30000,1,33,32,,
CTRIA3,32,30000,1,34,33,,
CTRIA3,33,30000,1,35,34,,
CTRIA3,34,30000,1,36,35,,
CTRIA3,35,30000,1,37,36,,
CTRIA3,36,30000,1,38,37,,
CTRIA3,37,30000,1,39,38,,
CTRIA3,38,30000,1,40,39,,
CTRIA3,39,30000,1,41,40,,
CTRIA3,40,30000,1,42,41,,
CTRIA3,41,30000,1,43,42,,
CTRIA3,42,30000,1,44,43,,
CTRIA3,43,30000,1,45,44,,
CTRIA3,44,30000,1,46,45,,
CTRIA3,45,30000,1,47,46,,
CTRIA3,46,30000,1,48,47,,
CTRIA3,47,30000,1,49,48,,
CTRIA3,48,30000,1,50,49,,
CTRIA3,49,30000,1,51,50,,
CTRIA3,50,30000,1,52,51,,
CTRIA3,51,30000,1,53,52,,
CTRIA3,52,30000,1,54,53,,
CTRIA3,53,30000,1,55,54,,
CTRIA3,54,30000,1,56,55,,
CTRIA3,55,30000,1,57,56,,
CTRIA3,56,30000,1,58,57,,
CTRIA3,57,30000,1,59,58,,
CTRIA3,58,30000,1,60,59,,
CTRIA3,59,30000,1,61,60,,
CTRIA3,60,30000,1,62,61,,
CTRIA3,61,30000,1,63,62,,
CTRIA3,62,30000,1,64,63,,
CTRIA3,63,30000,1,65,64,,
CTRIA3,64,30000,1,2,65,,
CQUAD4,65,30000,2,3,67,66,,
CQUAD4,66,30000,3,4,68,67,,
CQUAD4,67,30000,4,5,69,68,,
CQUAD4,68,30000,5,6,70,69,,
```

```
CQUAD4,69,30000,6,7,71,70,,
CQUAD4,70,30000,7,8,72,71,,
CQUAD4,71,30000,8,9,73,72,,
CQUAD4,72,30000,9,10,74,73,,
CQUAD4,73,30000,10,11,75,74,,
CQUAD4,74,30000,11,12,76,75,,
CQUAD4,75,30000,12,13,77,76,,
CQUAD4,76,30000,13,14,78,77,,
CQUAD4,77,30000,14,15,79,78,,
CQUAD4,78,30000,15,16,80,79,,
CQUAD4,79,30000,16,17,81,80,,
CQUAD4,80,30000,17,18,82,81,,
CQUAD4,81,30000,18,19,83,82,,
CQUAD4,82,30000,19,20,84,83,,
CQUAD4,83,30000,20,21,85,84,,
CQUAD4,84,30000,21,22,86,85,,
CQUAD4,85,30000,22,23,87,86,,
CQUAD4,86,30000,23,24,88,87,,
CQUAD4,87,30000,24,25,89,88,,
CQUAD4,88,30000,25,26,90,89,,
CQUAD4,89,30000,26,27,91,90,,
CQUAD4,90,30000,27,28,92,91,,
CQUAD4,91,30000,28,29,93,92,,
CQUAD4,92,30000,29,30,94,93,,
CQUAD4,93,30000,30,31,95,94,,
CQUAD4,94,30000,31,32,96,95,,
CQUAD4,95,30000,32,33,97,96,,
CQUAD4,96,30000,33,34,98,97,,
CQUAD4,97,30000,34,35,99,98,,
CQUAD4,98,30000,35,36,100,99,,
CQUAD4,99,30000,36,37,101,100,,
CQUAD4,100,30000,37,38,102,101,,
```


EXAMPLE SET OF LONGERON BAR ELEMENTS

```
CBAR,5057,20000,1,2,5058
CBAR,5058,20000,2,66,5058
CBAR,5059,20000,66,130,5058
CBAR,5060,20000,130,194,5058
CBAR,5061,20000,194,258,5058
CBAR,5062,20000,258,322,5058
CBAR,5063,20000,322,386,5058
CBAR,5064,20000,386,450,5058
CBAR,5065,20000,450,514,5058
CBAR,5066,20000,514,578,5058
CBAR,5067,20000,578,642,5058
CBAR,5068,20000,642,706,5058
CBAR,5069,20000,706,770,5058
CBAR,5070,20000,770,834,5058
CBAR,5071,20000,834,898,5058
CBAR,5072,20000,898,962,5058
CBAR,5073,20000,962,1026,5058
```

```
CBAR,5074,20000,1026,1090,5058
CBAR,5075,20000,1090,1154,5058
```


EXAMPLE SET OF FRAME RING BAR ELEMENTS

```
CBAR,6009,22002,4994,4995,5118
CBAR,6010,22002,4995,4996,5118
CBAR,6011,22002,4996,4997,5118
CBAR,6012,22002,4997,4998,5118
CBAR,6013,22002,4998,4999,5118
CBAR,6014,22002,4999,5000,5118
CBAR,6015,22002,5000,5001,5118
CBAR,6016,22002,5001,5002,5118
CBAR,6017,22002,5002,5003,5118
CBAR,6018,22002,5003,5004,5118
CBAR,6019,22002,5004,5005,5118
CBAR,6020,22002,5005,5006,5118
CBAR,6021,22002,5006,5007,5118
CBAR,6022,22002,5007,5008,5118
CBAR,6023,22002,5008,5009,5118
CBAR,6024,22002,5009,5010,5118
CBAR,6025,22002,5010,5011,5118
CBAR,6026,22002,5011,5012,5118
CBAR,6027,22002,5012,5013,5118
CBAR,6028,22002,5013,5014,5118
CBAR,6029,22002,5014,5015,5118
CBAR,6030,22002,5015,5016,5118
CBAR,6031,22002,5016,5017,5118
CBAR,6032,22002,5017,5018,5118
CBAR,6033,22002,5018,5019,5118
CBAR,6034,22002,5019,5020,5118
CBAR,6035,22002,5020,5021,5118
CBAR,6036,22002,5021,5022,5118
CBAR,6037,22002,5022,5023,5118
CBAR,6038,22002,5023,5024,5118
CBAR,6039,22002,5024,5025,5118
CBAR,6040,22002,5025,5026,5118
CBAR,6041,22002,5026,5027,5118
CBAR,6042,22002,5027,5028,5118
CBAR,6043,22002,5028,5029,5118
CBAR,6044,22002,5029,5030,5118
CBAR,6045,22002,5030,5031,5118
CBAR,6046,22002,5031,5032,5118
CBAR,6047,22002,5032,5033,5118
CBAR,6048,22002,5033,5034,5118
CBAR,6049,22002,5034,5035,5118
CBAR,6050,22002,5035,5036,5118
CBAR,6051,22002,5036,5037,5118
CBAR,6052,22002,5037,5038,5118
CBAR,6053,22002,5038,5039,5118
CBAR,6054,22002,5039,5040,5118
CBAR,6055,22002,5040,5041,5118
```

```
CBAR,6056,22002,5041,5042,5118
CBAR,6057,22002,5042,5043,5118
CBAR,6058,22002,5043,5044,5118
CBAR,6059,22002,5044,5045,5118
CBAR,6060,22002,5045,5046,5118
CBAR,6061,22002,5046,5047,5118
CBAR,6062,22002,5047,5048,5118
CBAR,6063,22002,5048,5049,5118
CBAR,6064,22002,5049,5050,5118
CBAR,6065,22002,5050,5051,5118
CBAR,6066,22002,5051,5052,5118
CBAR,6067,22002,5052,5053,5118
CBAR,6068,22002,5053,5054,5118
CBAR,6069,22002,5054,5055,5118
CBAR,6070,22002,5055,5056,5118
CBAR,6071,22002,5056,5057,5118
CBAR,6072,22002,5057,4994,5118
```

PAYLOAD MASS ELEMENTS AND THEIR ROD AND MPC LINKS

```
CONM2,6073,5070,,25000.0,0.0,0.0,0.0
,0.0,0.0,0.0,0.0,0.0,0.0
RBE3,6074,,5070,123456,1.0,123,1922,1930
,1938,1946,1954,1962,1970,1978
CONM2,6075,5082,,25000.0,0.0,0.0,0.0
,0.0,0.0,0.0,0.0,0.0,0.0
RBE3,6076,,5082,123456,1.0,123,2690,2698
,2706,2714,2722,2730,2738,2746
CONM2,6077,5094,,25000.0,0.0,0.0,0.0
,0.0,0.0,0.0,0.0,0.0,0.0
RBE3,6078,,5094,123456,1.0,123,3458,3466
,3474,3482,3490,3498,3506,3514
CONM2,6079,5106,,25000.0,0.0,0.0,0.0
,0.0,0.0,0.0,0.0,0.0,0.0
RBE3,6080,,5106,123456,1.0,123,4226,4234
,4242,4250,4258,4266,4274,4282
CROD,6081,10000,5070,5082
CROD,6082,10000,5082,5094
CROD,6083,10000,5094,5106
```

Loads

PARAM AND SPC CARDS

```
PARAM,POST,0
PARAM,PRTMAXIM,YES
SPC1,1,123456,4994,5002,5010,5018,5026,5034,5042,5050
SPC1,2,123456,5058,THRU,5069
SPC1,3,123456,5071,THRU,5081
SPC1,4,123456,5083,THRU,5093
SPC1,5,123456,5095,THRU,5105
SPC1,6,123456,5107,THRU,5118
SPCADD,7,1,2,3,4,5,6
```

EXAMPLE OF PRESSURE LOADS

```
PLOAD4,1,1,-3289.89928337,-1555.29906053,-1548.93089201
PLOAD4,1,2,-3289.89928337,-1574.4201813,-1555.29906053
PLOAD4,1,3,-3289.89928337,-1606.34094463,-1574.4201813
PLOAD4,1,4,-3289.89928337,-1651.12879532,-1606.34094463
PLOAD4,1,5,-3289.89928337,-1708.85687749,-1651.12879532
PLOAD4,1,6,-3289.89928337,-1779.58394347,-1708.85687749
PLOAD4,1,7,-3289.89928337,-1863.33016517,-1779.58394347
PLOAD4,1,8,-3289.89928337,-1960.04998881,-1863.33016517
PLOAD4,1,9,-3289.89928337,-2069.60333005,-1960.04998881
PLOAD4,1,10,-3289.89928337,-2191.72651072,-2069.60333005
PLOAD4,1,11,-3289.89928337,-2326.00438595,-2191.72651072
PLOAD4,1,12,-3289.89928337,-2471.84509864,-2326.00438595
PLOAD4,1,13,-3289.89928337,-2628.4588283,-2471.84509864
PLOAD4,1,14,-3289.89928337,-2794.84177472,-2628.4588283
PLOAD4,1,15,-3289.89928337,-2969.76643836,-2794.84177472
PLOAD4,1,16,-3289.89928337,-3151.77903624,-2969.76643836
PLOAD4,1,17,-3289.89928337,-3339.20463171,-3151.77903624
PLOAD4,1,18,-3289.89928337,-3530.16026967,-3339.20463171
PLOAD4,1,19,-3289.89928337,-3722.57610577,-3530.16026967
PLOAD4,1,20,-3289.89928337,-3914.22421115,-3722.57610577
PLOAD4,1,21,-3289.89928337,-4102.75443416,-3914.22421115
PLOAD4,1,22,-3289.89928337,-4285.73642038,-4102.75443416
PLOAD4,1,23,-3289.89928337,-4460.70664104,-4285.73642038
PLOAD4,1,24,-3289.89928337,-4625.21906915,-4460.70664104
PLOAD4,1,25,-3289.89928337,-4776.89797967,-4625.21906915
PLOAD4,1,26,-3289.89928337,-4913.49124136,-4776.89797967
PLOAD4,1,27,-3289.89928337,-5032.92241832,-4913.49124136
PLOAD4,1,28,-3289.89928337,-5133.34001082,-5032.92241832
PLOAD4,1,29,-3289.89928337,-5213.16223722,-5133.34001082
PLOAD4,1,30,-3289.89928337,-5271.11589024,-5213.16223722
PLOAD4,1,31,-3289.89928337,-5306.26798533,-5271.11589024
PLOAD4,1,32,-3289.89928337,-5318.04915144,-5306.26798533
PLOAD4,1,33,-3289.89928337,-5306.26798533,-5318.04915144
PLOAD4,1,34,-3289.89928337,-5271.11589024,-5306.26798533
PLOAD4,1,35,-3289.89928337,-5213.16223722,-5271.11589024
PLOAD4,1,36,-3289.89928337,-5133.34001082,-5213.16223722
PLOAD4,1,37,-3289.89928337,-5032.92241832,-5133.34001082
PLOAD4,1,38,-3289.89928337,-4913.49124136,-5032.92241832
PLOAD4,1,39,-3289.89928337,-4776.89797967,-4913.49124136
PLOAD4,1,40,-3289.89928337,-4625.21906915,-4776.89797967
PLOAD4,1,41,-3289.89928337,-4460.70664104,-4625.21906915
PLOAD4,1,42,-3289.89928337,-4285.73642038,-4460.70664104
PLOAD4,1,43,-3289.89928337,-4102.75443416,-4285.73642038
PLOAD4,1,44,-3289.89928337,-3914.22421115,-4102.75443416
PLOAD4,1,45,-3289.89928337,-3722.57610577,-3914.22421115
PLOAD4,1,46,-3289.89928337,-3530.16026967,-3722.57610577
PLOAD4,1,47,-3289.89928337,-3339.20463171,-3530.16026967
PLOAD4,1,48,-3289.89928337,-3151.77903624,-3339.20463171
PLOAD4,1,49,-3289.89928337,-2969.76643836,-3151.77903624
PLOAD4,1,50,-3289.89928337,-2794.84177472,-2969.76643836
PLOAD4,1,51,-3289.89928337,-2628.4588283,-2794.84177472
PLOAD4,1,52,-3289.89928337,-2471.84509864,-2628.4588283
PLOAD4,1,53,-3289.89928337,-2326.00438595,-2471.84509864
PLOAD4,1,54,-3289.89928337,-2191.72651072,-2326.00438595
PLOAD4,1,55,-3289.89928337,-2069.60333005,-2191.72651072
```

```
PLOAD4,1,56,-3289.89928337,-1960.04998881,-2069.60333005
PLOAD4,1,57,-3289.89928337,-1863.33016517,-1960.04998881
PLOAD4,1,58,-3289.89928337,-1779.58394347,-1863.33016517
PLOAD4,1,59,-3289.89928337,-1708.85687749,-1779.58394347
PLOAD4,1,60,-3289.89928337,-1651.12879532,-1708.85687749
PLOAD4,1,61,-3289.89928337,-1606.34094463,-1651.12879532
PLOAD4,1,62,-3289.89928337,-1574.4201813,-1606.34094463
PLOAD4,1,63,-3289.89928337,-1555.29906053,-1574.4201813
PLOAD4,1,64,-3289.89928337,-645.46057398,-1555.29906053
```



```
PLOAD4,1,5009,0.0,-64.466351868,-64.466351868,0.0
PLOAD4,1,5010,-64.466351868,-255.388001723,-255.388001723,-64.466351868
PLOAD4,1,5011,-255.388001723,-565.427937631,-565.427937631,-255.388001723
PLOAD4,1,5012,-565.427937631,-982.671498728,-982.671498728,-565.427937631
PLOAD4,1,5013,-982.671498728,-1491.08424895,-1491.08424895,-982.671498728
PLOAD4,1,5014,-1491.08424895,-2071.12817144,-2071.12817144,-1491.08424895
PLOAD4,1,5015,-2071.12817144,-2700.51250353,-2700.51250353,-2071.12817144
PLOAD4,1,5016,-2700.51250353,-3355.05035831,-3355.05035831,-2700.51250353
PLOAD4,1,5017,-3355.05035831,-4009.5882131,-4009.5882131,-3355.05035831
PLOAD4,1,5018,-4009.5882131,-4638.97254519,-4638.97254519,-4009.5882131
PLOAD4,1,5019,-4638.97254519,-5219.01646768,-5219.01646768,-4638.97254519
PLOAD4,1,5020,-5219.01646768,-5727.4292179,-5727.4292179,-5219.01646768
PLOAD4,1,5021,-5727.4292179,-6144.672779,-6144.672779,-5727.4292179
PLOAD4,1,5022,-6144.672779,-6454.71271491,-6454.71271491,-6144.672779
PLOAD4,1,5023,-6454.71271491,-6645.63436476,-6645.63436476,-6454.71271491
PLOAD4,1,5024,-6645.63436476,-6710.10071663,-6710.10071663,-6645.63436476
PLOAD4,1,5025,-6710.10071663,-6645.63436476,-6645.63436476,-6710.10071663
PLOAD4,1,5026,-6645.63436476,-6454.71271491,-6454.71271491,-6645.63436476
PLOAD4,1,5027,-6454.71271491,-6144.672779,-6144.672779,-6454.71271491
PLOAD4,1,5028,-6144.672779,-5727.4292179,-5727.4292179,-6144.672779
PLOAD4,1,5029,-5727.4292179,-5219.01646768,-5219.01646768,-5727.4292179
PLOAD4,1,5030,-5219.01646768,-4638.97254519,-4638.97254519,-5219.01646768
PLOAD4,1,5031,-4638.97254519,-4009.5882131,-4009.5882131,-4638.97254519
PLOAD4,1,5032,-4009.5882131,-3355.05035831,-3355.05035831,-4009.5882131
PLOAD4,1,5033,-3355.05035831,-2700.51250353,-2700.51250353,-3355.05035831
PLOAD4,1,5034,-2700.51250353,-2071.12817144,-2071.12817144,-2700.51250353
PLOAD4,1,5035,-2071.12817144,-1491.08424895,-1491.08424895,-2071.12817144
PLOAD4,1,5036,-1491.08424895,-982.671498728,-982.671498728,-1491.08424895
PLOAD4,1,5037,-982.671498728,-565.427937631,-565.427937631,-982.671498728
PLOAD4,1,5038,-565.427937631,-255.388001723,-255.388001723,-565.427937631
PLOAD4,1,5039,-255.388001723,-64.466351868,-64.466351868,-255.388001723
PLOAD4,1,5040,-64.466351868,-0.0,-0.0,-64.466351868
PLOAD4,1,5041,-0.0,0.0,0.0,-0.0
PLOAD4,1,5042,0.0,0.0,0.0,0.0
PLOAD4,1,5043,0.0,0.0,0.0,0.0
PLOAD4,1,5044,0.0,0.0,0.0,0.0
PLOAD4,1,5045,0.0,0.0,0.0,0.0
PLOAD4,1,5046,0.0,0.0,0.0,0.0
PLOAD4,1,5047,0.0,0.0,0.0,0.0
PLOAD4,1,5048,0.0,0.0,0.0,0.0
PLOAD4,1,5049,0.0,0.0,0.0,0.0
PLOAD4,1,5050,0.0,0.0,0.0,0.0
```

```
PLOAD4,1,5051,0.0,0.0,0.0,0.0
PLOAD4,1,5052,0.0,0.0,0.0,0.0
PLOAD4,1,5053,0.0,0.0,0.0,0.0
PLOAD4,1,5054,0.0,0.0,0.0,0.0
PLOAD4,1,5055,0.0,0.0,0.0,0.0
PLOAD4,1,5056,0.0,0.0,0.0,0.0
PLOAD4,2,1,-55773.0978596,-51501.5650879,-51492.3129268
PLOAD4,2,2,-55773.0978596,-51529.2374266,-51501.5650879
PLOAD4,2,3,-55773.0978596,-51575.0781293,-51529.2374266
PLOAD4,2,4,-55773.0978596,-51638.6695737,-51575.0781293
PLOAD4,2,5,-55773.0978596,-51719.4314347,-51638.6695737
PLOAD4,2,6,-55773.0978596,-51816.6250394,-51719.4314347
PLOAD4,2,7,-55773.0978596,-51929.3589784,-51816.6250394
PLOAD4,2,8,-55773.0978596,-52056.5959757,-51929.3589784
PLOAD4,2,9,-55773.0978596,-52197.1610175,-52056.5959757
PLOAD4,2,10,-55773.0978596,-52349.7507342,-52197.1610175
PLOAD4,2,11,-55773.0978596,-52512.9440165,-52349.7507342
PLOAD4,2,12,-55773.0978596,-52685.2138423,-52512.9440165
PLOAD4,2,13,-55773.0978596,-52864.9402667,-52685.2138423
PLOAD4,2,14,-55773.0978596,-53050.4245214,-52864.9402667
PLOAD4,2,15,-55773.0978596,-53239.9041404,-53050.4245214
PLOAD4,2,16,-55773.0978596,-53431.5690175,-53239.9041404
PLOAD4,2,17,-55773.0978596,-53623.5782739,-53431.5690175
PLOAD4,2,18,-55773.0978596,-53814.0777967,-53623.5782739
PLOAD4,2,19,-55773.0978596,-54001.2182853,-53814.0777967
PLOAD4,2,20,-55773.0978596,-54183.1736256,-54001.2182853
PLOAD4,2,21,-55773.0978596,-54358.1593932,-54183.1736256
PLOAD4,2,22,-55773.0978596,-54524.4512713,-54358.1593932
PLOAD4,2,23,-55773.0978596,-54680.4031601,-54524.4512713
PLOAD4,2,24,-55773.0978596,-54824.4647445,-54680.4031601
PLOAD4,2,25,-55773.0978596,-54955.1982841,-54824.4647445
PLOAD4,2,26,-55773.0978596,-55071.2943954,-54955.1982841
PLOAD4,2,27,-55773.0978596,-55171.5865958,-55071.2943954
PLOAD4,2,28,-55773.0978596,-55255.0643986,-55171.5865958
PLOAD4,2,29,-55773.0978596,-55320.884759,-55255.0643986
PLOAD4,2,30,-55773.0978596,-55368.3816955,-55320.884759
PLOAD4,2,31,-55773.0978596,-55397.0739381,-55368.3816955
PLOAD4,2,32,-55773.0978596,-55406.6704785,-55397.0739381
PLOAD4,2,33,-55773.0978596,-55397.0739381,-55406.6704785
PLOAD4,2,34,-55773.0978596,-55368.3816955,-55397.0739381
PLOAD4,2,35,-55773.0978596,-55320.884759,-55368.3816955
PLOAD4,2,36,-55773.0978596,-55255.0643986,-55320.884759
PLOAD4,2,37,-55773.0978596,-55171.5865958,-55255.0643986
PLOAD4,2,38,-55773.0978596,-55071.2943954,-55171.5865958
PLOAD4,2,39,-55773.0978596,-54955.1982841,-55071.2943954
PLOAD4,2,40,-55773.0978596,-54824.4647445,-54955.1982841
PLOAD4,2,41,-55773.0978596,-54680.4031601,-54824.4647445
PLOAD4,2,42,-55773.0978596,-54524.4512713,-54680.4031601
PLOAD4,2,43,-55773.0978596,-54358.1593932,-54524.4512713
PLOAD4,2,44,-55773.0978596,-54183.1736256,-54358.1593932
PLOAD4,2,45,-55773.0978596,-54001.2182853,-54183.1736256
PLOAD4,2,46,-55773.0978596,-53814.0777967,-54001.2182853
PLOAD4,2,47,-55773.0978596,-53623.5782739,-53814.0777967
PLOAD4,2,48,-55773.0978596,-53431.5690175,-53623.5782739
PLOAD4,2,49,-55773.0978596,-53239.9041404,-53431.5690175
PLOAD4,2,50,-55773.0978596,-53050.4245214,-53239.9041404
PLOAD4,2,51,-55773.0978596,-52864.9402667,-53050.4245214
```

```
PLOAD4,2,52,-55773.0978596,-52685.2138423,-52864.9402667
PLOAD4,2,53,-55773.0978596,-52512.9440165,-52685.2138423
PLOAD4,2,54,-55773.0978596,-52349.7507342,-52512.9440165
PLOAD4,2,55,-55773.0978596,-52197.1610175,-52349.7507342
PLOAD4,2,56,-55773.0978596,-52056.5959757,-52197.1610175
PLOAD4,2,57,-55773.0978596,-51929.3589784,-52056.5959757
PLOAD4,2,58,-55773.0978596,-51816.6250394,-51929.3589784
PLOAD4,2,59,-55773.0978596,-51719.4314347,-51816.6250394
PLOAD4,2,60,-55773.0978596,-51638.6695737,-51719.4314347
PLOAD4,2,61,-55773.0978596,-51575.0781293,-51638.6695737
PLOAD4,2,62,-55773.0978596,-51529.2374266,-51575.0781293
PLOAD4,2,63,-55773.0978596,-51501.5650879,-51529.2374266
PLOAD4,2,64,-55773.0978596,-45949.4483006,-51501.5650879
```



```
PLOAD4,2,5009,0.0,-4.10140246111,-4.10140246111,0.0
PLOAD4,2,5010,-4.10140246111,-16.247995248,-16.247995248,-4.10140246111
PLOAD4,2,5011,-16.247995248,-35.9729916116,-35.9729916116,-16.247995248
PLOAD4,2,5012,-35.9729916116,-62.5183710038,-62.5183710038,-35.9729916116
PLOAD4,2,5013,-62.5183710038,-94.8640093811,-94.8640093811,-62.5183710038
PLOAD4,2,5014,-94.8640093811,-131.766882001,-131.766882001,-94.8640093811
PLOAD4,2,5015,-131.766882001,-171.808832163,-171.808832163,-131.766882001
PLOAD4,2,5016,-171.808832163,-213.451070178,-213.451070178,-171.808832163
PLOAD4,2,5017,-213.451070178,-255.093308194,-255.093308194,-213.451070178
PLOAD4,2,5018,-255.093308194,-295.135258356,-295.135258356,-255.093308194
PLOAD4,2,5019,-295.135258356,-332.038130976,-332.038130976,-295.135258356
PLOAD4,2,5020,-332.038130976,-364.383769353,-364.383769353,-332.038130976
PLOAD4,2,5021,-364.383769353,-390.929148745,-390.929148745,-364.383769353
PLOAD4,2,5022,-390.929148745,-410.654145109,-410.654145109,-390.929148745
PLOAD4,2,5023,-410.654145109,-422.800737896,-422.800737896,-410.654145109
PLOAD4,2,5024,-422.800737896,-426.902140357,-426.902140357,-422.800737896
PLOAD4,2,5025,-426.902140357,-422.800737896,-422.800737896,-426.902140357
PLOAD4,2,5026,-422.800737896,-410.654145109,-410.654145109,-422.800737896
PLOAD4,2,5027,-410.654145109,-390.929148745,-390.929148745,-410.654145109
PLOAD4,2,5028,-390.929148745,-364.383769353,-364.383769353,-390.929148745
PLOAD4,2,5029,-364.383769353,-332.038130976,-332.038130976,-364.383769353
PLOAD4,2,5030,-332.038130976,-295.135258356,-295.135258356,-332.038130976
PLOAD4,2,5031,-295.135258356,-255.093308194,-255.093308194,-295.135258356
PLOAD4,2,5032,-255.093308194,-213.451070178,-213.451070178,-255.093308194
PLOAD4,2,5033,-213.451070178,-171.808832163,-171.808832163,-213.451070178
PLOAD4,2,5034,-171.808832163,-131.766882001,-131.766882001,-171.808832163
PLOAD4,2,5035,-131.766882001,-94.8640093811,-94.8640093811,-131.766882001
PLOAD4,2,5036,-94.8640093811,-62.5183710038,-62.5183710038,-94.8640093811
PLOAD4,2,5037,-62.5183710038,-35.9729916116,-35.9729916116,-62.5183710038
PLOAD4,2,5038,-35.9729916116,-16.247995248,-16.247995248,-35.9729916116
PLOAD4,2,5039,-16.247995248,-4.10140246111,-4.10140246111,-16.247995248
PLOAD4,2,5040,-4.10140246111,0.0,0.0,-4.10140246111
PLOAD4,2,5041,0.0,0.0,0.0,0.0
PLOAD4,2,5042,0.0,0.0,0.0,0.0
PLOAD4,2,5043,0.0,0.0,0.0,0.0
PLOAD4,2,5044,0.0,0.0,0.0,0.0
PLOAD4,2,5045,0.0,0.0,0.0,0.0
PLOAD4,2,5046,0.0,0.0,0.0,0.0
```

```
PLOAD4,2,5047,0.0,0.0,0.0,0.0
PLOAD4,2,5048,0.0,0.0,0.0,0.0
PLOAD4,2,5049,0.0,0.0,0.0,0.0
PLOAD4,2,5050,0.0,0.0,0.0,0.0
PLOAD4,2,5051,0.0,0.0,0.0,0.0
PLOAD4,2,5052,0.0,0.0,0.0,0.0
PLOAD4,2,5053,0.0,0.0,0.0,0.0
PLOAD4,2,5054,0.0,0.0,0.0,0.0
PLOAD4,2,5055,0.0,0.0,0.0,0.0
PLOAD4,2,5056,0.0,0.0,0.0,0.0
```

LOAD AND GRAVITY CARDS

```
$ Entry Loads
LOAD,3,1.0,1.0,1
GRAV,4,0,7.3575,0.0,1.0,0.0,0
GRAV,5,0,39.24,1.0,0.0,0.0,0
$ Launch Loads Case: 1
LOAD,6,1.0,0.1,2,1.0,4,1.0,5
$
ENDDATA
```

B.2: Frequency Response (SOL 111)

```
BEGIN BULK
PARAM,POST,0
PARAM,K6ROT,1.0
PARAM,GRDPNT,0
$ Need to put full constraints on reference grid points to prevent
singularity
SPC1,1,123456,4994,5002,5010,5018,5026,5034,5042,5050
SPC1,2,123456,5058,THRU,5069
SPC1,3,123456,5071,THRU,5081
SPC1,4,123456,5083,THRU,5093
SPC1,5,123456,5095,THRU,5105
SPC1,6,123456,5107,THRU,5118
SPCADD,7,1,2,3,4,5,6
FREQ1,8,10.0,1.0,300
FREQ4,8,10.0,250.0,0.1,5
EIGRL,9,0.0,300.0
TABDMP1,2,CRIT
,0.0,0.005,8.0,0.005,1000.0,0.005,ENDT
TABLED1,3
,0.0,1.0,1.001,1.0,400.0,1.0,ENDT
PLOAD4,10,1,-1.0,,,,THRU,5056
RLOAD1,11,10,,,3
DLOAD,12,1.0,1.0,11
INCLUDE DeltaIV_Heavy_Vibes.dat'
RANDPS,13,1,1,1.0,0.0,1
INCLUDE 'Nodes_1.dat'
INCLUDE 'Elements_1.dat'
$
ENDDATA
```

B.3: Design Optimization (SOL 200)

```
BEGIN BULK
PARAM,GRDPNT,0
PARAM,NASPRT,1
$ Real Eigenvalue Extraction Data, Lanczos Method - for buckling and modes
subcases
EIGRL,1,,,10
INCLUDE 'Nodes_1.dat'
INCLUDE 'Elements_1.dat'
INCLUDE 'Loads_1.dat'
DESVAR,1,Core_0,0.1,1.00E-02,1.00E-01
DESVAR,2,Lam_0,0.02,1.00E-03,2.00E-02
DESVAR,3,Core_1,0.1,1.00E-02,1.00E-01
DESVAR,4,Lam_1,0.02,1.00E-03,2.00E-02
DESVAR,5,Core_2,0.1,1.00E-02,1.00E-01
DESVAR,6,Lam_2,0.02,1.00E-03,2.00E-02
DESVAR,7,Core_3,0.1,1.00E-02,1.00E-01
DESVAR,8,Lam_3,0.02,1.00E-03,2.00E-02
DESVAR,9,Core_4,0.1,1.00E-02,1.00E-01
DESVAR,10,Lam_4,0.02,1.00E-03,2.00E-02
DESVAR,11,Core_5,0.1,1.00E-02,1.00E-01
DESVAR,12,Lam_5,0.02,1.00E-03,2.00E-02
DESVAR,13,ldim1,0.04,5.00E-03,0.04
DESVAR,14,ldim2,0.04,5.00E-03,0.04
DESVAR,15,ldim3,0.3,0.05,3.00E-01
DESVAR,16,ldim4,0.3,0.05,3.00E-01
DESVAR,17,fdim1_0,0.02,5.00E-03,0.04
DESVAR,18,fdim2_0,0.02,5.00E-03,0.04
DESVAR,19,fdim3_0,0.15,0.04,3.00E-01
DESVAR,20,fdim4_0,0.15,0.04,3.00E-01
DESVAR,21,fdim1_1,0.04,5.00E-03,0.04
DESVAR,22,fdim2_1,0.04,5.00E-03,0.04
DESVAR,23,fdim3_1,0.3,0.04,3.00E-01
DESVAR,24,fdim4_1,0.3,0.04,3.00E-01
DESVAR,25,fdim1_2,0.04,5.00E-03,0.04
DESVAR,26,fdim2_2,0.04,5.00E-03,0.04
DESVAR,27,fdim3_2,0.3,0.04,3.00E-01
DESVAR,28,fdim4_2,0.3,0.04,3.00E-01
DEQATN  1       RATIO(D,W)=D/W
DRESP1,1,total_W,WEIGHT
DRESP1,13,CF_Stress,CSTRESS,PCOMP,,9,2,30000
DCONSTR,1,13,,5.12E+08
DRESP1,14,HC_Stress,CSTRESS,PCOMP,,9,2,30000
DCONSTR,1,14,,1.48E+06
DRESP1,15,CF_Stress,CSTRESS,PCOMP,,9,2,30001
DCONSTR,1,15,,5.12E+08
DRESP1,16,HC_Stress,CSTRESS,PCOMP,,9,2,30001
DCONSTR,1,16,,1.48E+06
DRESP1,17,CF_Stress,CSTRESS,PCOMP,,9,2,30002
DCONSTR,1,17,,5.12E+08
DRESP1,18,HC_Stress,CSTRESS,PCOMP,,9,2,30002
DCONSTR,1,18,,1.48E+06
```

```
DRESP1,19,CF_Stress,CSTRESS,PCOMP,,9,2,30003
DCONSTR,1,19,,5.12E+08
DRESP1,20,HC_Stress,CSTRESS,PCOMP,,9,2,30003
DCONSTR,1,20,,1.48E+06
DRESP1,21,CF_Stress,CSTRESS,PCOMP,,9,2,30004
DCONSTR,1,21,,5.12E+08
DRESP1,22,HC_Stress,CSTRESS,PCOMP,,9,2,30004
DCONSTR,1,22,,1.48E+06
DRESP1,23,CF_Stress,CSTRESS,PCOMP,,9,2,30005
DCONSTR,1,23,,5.12E+08
DRESP1,24,HC_Stress,CSTRESS,PCOMP,,9,2,30005
DCONSTR,1,24,,1.48E+06
DRESP1,25,stressL,STRESS,PBARL,,7,,20000
DCONSTR,1,25,,5.12E+08
DRESP1,26,stressL,STRESS,PBARL,,14,,20000
DCONSTR,1,26,,5.12E+08
DRESP1,31,stressR,STRESS,PBARL,,7,,22000
DCONSTR,1,31,,5.12E+08
DRESP1,32,stressR,STRESS,PBARL,,14,,22000
DCONSTR,1,32,,5.12E+08
DRESP1,37,stressR,STRESS,PBARL,,7,,22001
DCONSTR,1,37,,5.12E+08
DRESP1,38,stressR,STRESS,PBARL,,14,,22001
DCONSTR,1,38,,5.12E+08
DRESP1,43,stressR,STRESS,PBARL,,7,,22002
DCONSTR,1,43,,5.12E+08
DRESP1,44,stressR,STRESS,PBARL,,14,,22002
DCONSTR,1,44,,5.12E+08
DRESP1,2,buck,LAMA,,,1
DCONSTR,2,2,1.0
DRESP1,3,buck,LAMA,,,2
DCONSTR,2,3,1.0
DRESP1,4,buck,LAMA,,,3
DCONSTR,2,4,1.0
DRESP1,5,buck,LAMA,,,4
DCONSTR,2,5,1.0
DRESP1,6,buck,LAMA,,,5
DCONSTR,2,6,1.0
DRESP1,7,buck,LAMA,,,6
DCONSTR,2,7,1.0
DRESP1,8,buck,LAMA,,,7
DCONSTR,2,8,1.0
DRESP1,9,buck,LAMA,,,8
DCONSTR,2,9,1.0
DRESP1,10,buck,LAMA,,,9
DCONSTR,2,10,1.0
DRESP1,11,buck,LAMA,,,10
DCONSTR,2,11,1.0
DRESP1,12,freq,FREQ,,,1
DCONSTR,3,12,7.0,1000.0
DRESP2,27,ratio1L,1
,DESVAR,13,16
DCONSTR,1,27,,0.5
DRESP2,28,ratio2L,1
,DESVAR,14,15
DCONSTR,1,28,,1.0
DRESP2,29,ratio3L,1
```

```
,DESVAR,14,16
DCONSTR,1,29,,0.125
DRESP2,30,ratio4L,1
,DESVAR,13,15
DCONSTR,1,30,,0.125
DRESP2,33,ratio1R,1
,DESVAR,17,20
DCONSTR,1,33,,0.5
DRESP2,34,ratio2R,1
,DESVAR,18,19
DCONSTR,1,34,,1.0
DRESP2,35,ratio4R,1
,DESVAR,18,20
DCONSTR,1,35,,0.125
DRESP2,36,ratio5R,1
,DESVAR,17,19
DCONSTR,1,36,,0.125
DRESP2,39,ratio1R,1
,DESVAR,21,24
DCONSTR,1,39,,0.5
DRESP2,40,ratio2R,1
,DESVAR,22,23
DCONSTR,1,40,,1.0
DRESP2,41,ratio4R,1
,DESVAR,22,24
DCONSTR,1,41,,0.125
DRESP2,42,ratio5R,1
,DESVAR,21,23
DCONSTR,1,42,,0.125
DRESP2,45,ratio1R,1
,DESVAR,25,28
DCONSTR,1,45,,0.5
DRESP2,46,ratio2R,1
,DESVAR,26,27
DCONSTR,1,46,,1.0
DRESP2,47,ratio4R,1
,DESVAR,26,28
DCONSTR,1,47,,0.125
DRESP2,48,ratio5R,1
,DESVAR,25,27
DCONSTR,1,48,,0.125
DVPREL1,1,PCOMP,30000,T2
,1,1.0
DVPREL1,2,PCOMP,30000,T1
,2,1.0
DVPREL1,3,PCOMP,30001,T2
,3,1.0
DVPREL1,4,PCOMP,30001,T1
,4,1.0
DVPREL1,5,PCOMP,30002,T2
,5,1.0
DVPREL1,6,PCOMP,30002,T1
,6,1.0
DVPREL1,7,PCOMP,30003,T2
,7,1.0
DVPREL1,8,PCOMP,30003,T1
,8,1.0
```

```
DVPREL1,9,PCOMP,30004,T2
,9,1.0
DVPREL1,10,PCOMP,30004,T1
,10,1.0
DVPREL1,11,PCOMP,30005,T2
,11,1.0
DVPREL1,12,PCOMP,30005,T1
,12,1.0
DVPREL1,13,PBARL,20000,DIM1
,13,1.0
DVPREL1,14,PBARL,20000,DIM2
,14,1.0
DVPREL1,15,PBARL,20000,DIM3
,15,1.0
DVPREL1,16,PBARL,20000,DIM4
,16,1.0
DVPREL1,17,PBARL,22000,DIM1
,17,1.0
DVPREL1,18,PBARL,22000,DIM2
,18,1.0
DVPREL1,19,PBARL,22000,DIM3
,19,1.0
DVPREL1,20,PBARL,22000,DIM4
,20,1.0
DVPREL1,21,PBARL,22001,DIM1
,21,1.0
DVPREL1,22,PBARL,22001,DIM2
,22,1.0
DVPREL1,23,PBARL,22001,DIM3
,23,1.0
DVPREL1,24,PBARL,22001,DIM4
,24,1.0
DVPREL1,25,PBARL,22002,DIM1
,25,1.0
DVPREL1,26,PBARL,22002,DIM2
,26,1.0
DVPREL1,27,PBARL,22002,DIM3
,27,1.0
DVPREL1,28,PBARL,22002,DIM4
,28,1.0
DOPTPRM,DESMAX,50,P1,1,P2,1
$
ENDDATA
```

Appendix C: Vibroacoustics Results

X Y - O U T P U T S U M M A R Y (A U T O O R P S D F)

PLOT TYPE	CURVE TYPE	FRAME NO.	CURVE ID./ PANEL : GRID ID	RMS VALUE	NO. POSITIVE CROSSINGS	XMIN FOR ALL DATA	XMAX FOR ALL DATA	YMIN FOR ALL DATA	X FOR YMIN	YMAX FOR ALL DATA	X FOR* YMAX
PSDF	PLYSIG	1	68(9)	1.782960E+01	1.724960E+02	1.000E+01	3.100E+02	1.059E-04	3.202E+01	3.613E+01	1.675E+02

XYPAPLOT FRAME 1

X-AXIS TITLE = FREQUENCY (HZ)

```
                +----------------------------------------------------------------------------------------------------------------------------+
                I                                                                                                                            I
                I X-DIR PSDF OF ELEMENT STRESS PSI^2/HZ 68                                                                                   I
                I                                                                                                                            I
                I  1.000000E-04                                      5.000005E+01                                      1.000000E+02 I
                +----------------------------------------------------------------------------------------------------------------------------+
 1.0000E+01 *                                                        I                                                                       I
 1.2475E+01 *                                                        I                                                                       I
 1.4950E+01 *                                                        I                                                                       I
 1.7425E+01 *                                                        I                                                                       I
 1.9900E+01 *                                                        I                                                                       I
 2.2375E+01 *                                                        I                                                                       I
 2.4850E+01 *                                                        I                                                                       I
 2.7325E+01 *                                                        I                                                                       I
 2.9800E+01 **    *                                                  I                                                                       I
 3.2275E+01 *                                                        I                                                                       I
 3.4750E+01 *                                                        I                                                                       I
 3.7225E+01 *                                                        I                                                                       I
 3.9700E+01 *                                                        I                                                                       I
 4.2175E+01 *                                                        I                                                                       I
 4.4650E+01 *                                                        I                                                                       I
 4.7125E+01 *                                                        I                                                                       I
 4.9600E+01 *                                                        I                                                                       I
 5.2075E+01 *                                                        I                                                                       I
 5.4550E+01 *                                                        I                                                                       I
 5.7025E+01 *                                                        I                                                                       I
 5.9500E+01 *                                                        I                                                                       I
 6.1975E+01 *                                                        I                                                                       I
 6.4450E+01 *                                                        I                                                                       I
 6.6925E+01 *                                                        I                                                                       I
 6.9400E+01 *                                                        I                                                                       I
 7.1875E+01 *                                                        I                                                                       I
 7.4350E+01 *                                                        I                                                                       I
 7.6825E+01 *                                                        I                                                                       I
 7.9300E+01 *                                                        I                                                                       I
 8.1775E+01 *                                                        I                                                                       I
 8.4250E+01 **                                                       I                                                                       I
 8.6725E+01 *                                                        I                                                                       I
 8.9200E+01 *                                                        I                                                                       I
 9.1675E+01 *                                                        I                                                                       I
 9.4150E+01 *                                                        I                                                                       I
 9.6625E+01 *                                                        I                                                                       I
 9.9100E+01 *                                                        I                                                                       I
 1.0158E+02 *                                                        I                                                                       I
 1.0405E+02 *                                                        I                                                                       I
 1.0653E+02 *                                                        I                                                                       I
 1.0900E+02 *                                                        I                                                                       I
 1.1148E+02 **                                                       I                                                                       I
 1.1395E+02 *                                                        I                                                                       I
 1.1643E+02 *                                                        I                                                                       I
 1.1890E+02 *                                                        I                                                                       I
 1.2138E+02 *                                                        I                                                                       I
 1.2385E+02 I***       *       *                                     I                                                                       I
 1.2633E+02 **  *  *  * *    *     **  * *                           I                                                                       I
 1.2880E+02 *                                                        I                                                                       I
 1.3128E+02 **                                                       I                                                                       I
 1.3375E+02 ***                                                      I                                                                       I
 1.3623E+02 I******                                                  I                                                                       I
 1.3870E+02 I*                                                       I                                                                       I
 1.4118E+02 **                                                       I                                                                       I
 1.4365E+02 **                                                       I                                                                       I
 1.4612E+02 I****                                                    I                                                                       I
 1.4860E+02 **                                                       I                                                                       I
 1.5108E+02 *                                                        I                                                                       I
 1.5355E+02 *                                                        I                                                                       I
 1.5603E+02 **                                                       I                                                                       I
 1.5850E+02 **                                                       I                                                                       I
```

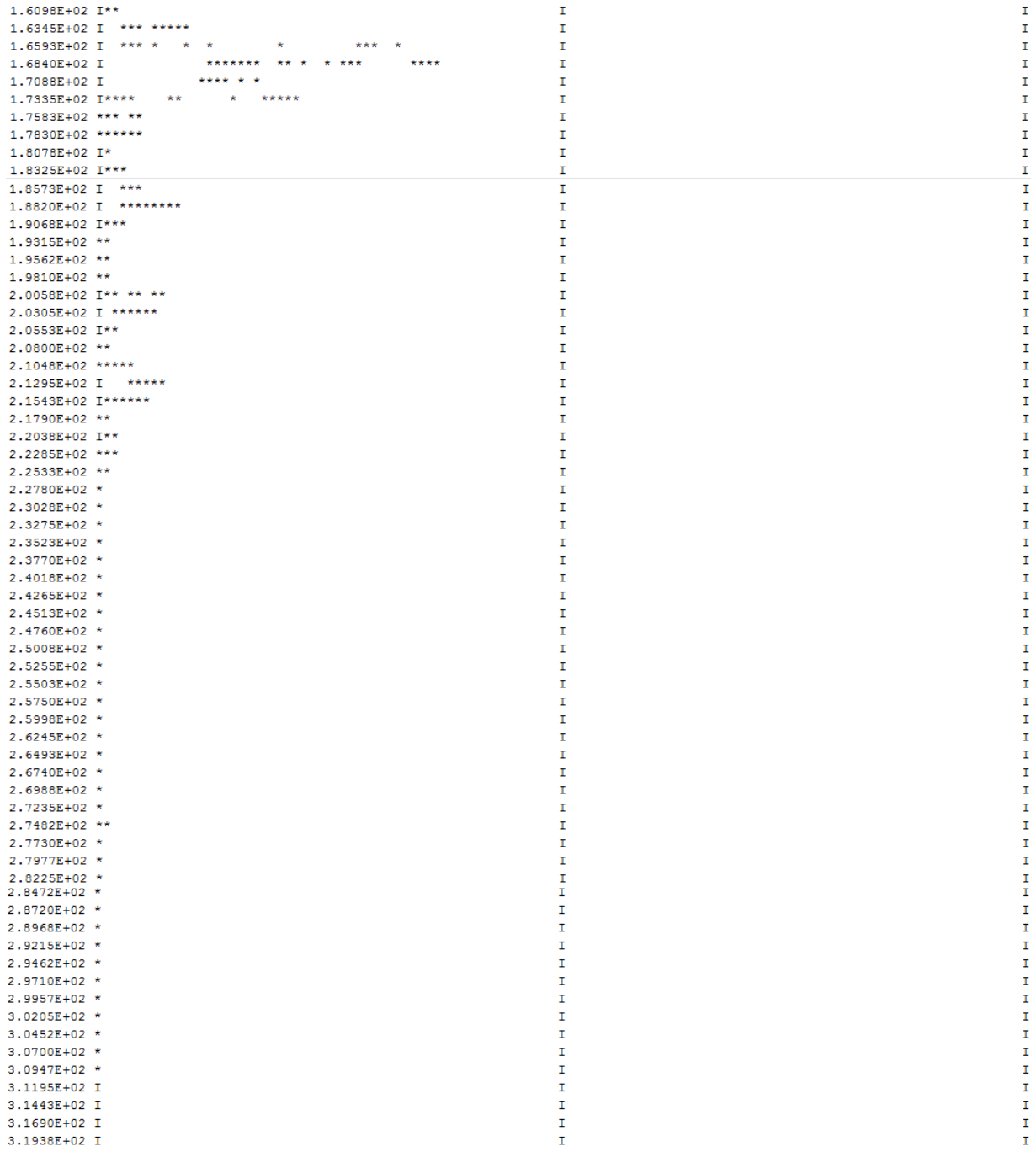
1.6098E+02 I**
1.6345E+02 I *** *****
1.6593E+02 I *** * * * * *** *
1.6840E+02 I ******* ** * * *** ****
1.7088E+02 I **** * *
1.7335E+02 I**** ** * *****
1.7583E+02 *** **
1.7830E+02 ******
1.8078E+02 I*
1.8325E+02 I***
1.8573E+02 I ***
1.8820E+02 I ********
1.9068E+02 I***
1.9315E+02 **
1.9562E+02 **
1.9810E+02 **
2.0058E+02 I** ** **
2.0305E+02 I ******
2.0553E+02 I**
2.0800E+02 **
2.1048E+02 *****
2.1295E+02 I *****
2.1543E+02 I******
2.1790E+02 **
2.2038E+02 I**
2.2285E+02 ***
2.2533E+02 **
2.2780E+02 *
2.3028E+02 *
2.3275E+02 *
2.3523E+02 *
2.3770E+02 *
2.4018E+02 *
2.4265E+02 *
2.4513E+02 *
2.4760E+02 *
2.5008E+02 *
2.5255E+02 *
2.5503E+02 *
2.5750E+02 *
2.5998E+02 *
2.6245E+02 *
2.6493E+02 *
2.6740E+02 *
2.6988E+02 *
2.7235E+02 *
2.7482E+02 **
2.7730E+02 *
2.7977E+02 *
2.8225E+02 *
2.8472E+02 *
2.8720E+02 *
2.8968E+02 *
2.9215E+02 *
2.9462E+02 *
2.9710E+02 *
2.9957E+02 *
3.0205E+02 *
3.0452E+02 *
3.0700E+02 *
3.0947E+02 *
3.1195E+02 I
3.1443E+02 I
3.1690E+02 I
3.1938E+02 I

REPORT DOCUMENTATION PAGE

Form Approved
OMB No. 0704-0188

1. REPORT DATE *(DD-MM-YYYY)*
01-02-2017

2. REPORT TYPE
Technical Memorandum

3. DATES COVERED *(From - To)*

4. TITLE AND SUBTITLE
Finite Element Modeling and Analysis of Mars Entry Aeroshell Baseline Concept

5a. CONTRACT NUMBER

5b. GRANT NUMBER

5c. PROGRAM ELEMENT NUMBER

6. AUTHOR(S)
Samee, Ahmed; Lane, Brittney

5d. PROJECT NUMBER

5e. TASK NUMBER

5f. WORK UNIT NUMBER
388496.04.01.02

7. PERFORMING ORGANIZATION NAME(S) AND ADDRESS(ES)
NASA Langley Research Center
Hampton, VA 23681-2199

8. PERFORMING ORGANIZATION REPORT NUMBER
L-20766

9. SPONSORING/MONITORING AGENCY NAME(S) AND ADDRESS(ES)
National Aeronautics and Space Administration
Washington, DC 20546-0001

10. SPONSOR/MONITOR'S ACRONYM(S)
NASA

11. SPONSOR/MONITOR'S REPORT NUMBER(S)
NASA-TM-2017-219374

12. DISTRIBUTION/AVAILABILITY STATEMENT
Unclassified - Unlimited
Subject Category 39
Availability: NASA STI Program (757) 864-9658

13. SUPPLEMENTARY NOTES

14. ABSTRACT

The structure that is developed and analyzed in this project must be able to survive all the various load conditions that it will encounter along its course to Mars with the minimal amount of weight and material. At this stage, the goal is to study the capability of the structure using a finite element (FE) model developed in Nastran & Patran. The purpose of the FE model is to achieve an optimization of mass given specific constraints on launch and entry. The generation and analysis of the baseline Rigid Mid-Range Lift to Drag Ratio Aeroshell model is a continuation and an improvement on previous work done for the finite element model. The model is generated using Python programming with the axisymmetric placement of nodes for beam and shell elements. The shells are assigned a honeycomb sandwich material with an aluminum honeycomb core and composite face sheets, and the beams are assigned the same material as the shell face sheets. There are two load cases assigned to the model: Earth launch and Mars entry. The Earth launch case consists of pressure, gravity, and vibration loads, and the Mars entry case consists of just pressure and gravity loads.

15. SUBJECT TERMS
Analysis; Finite element Modeling; Marsh entry aeroshell baseline concept

16. SECURITY CLASSIFICATION OF:			17. LIMITATION OF ABSTRACT	18. NUMBER OF PAGES	19a. NAME OF RESPONSIBLE PERSON
a. REPORT	b. ABSTRACT	c. THIS PAGE			STI Help Desk (email: help@sti.nasa.gov)
U	U	U	UU	76	19b. TELEPHONE NUMBER *(Include area code)* (757) 864-9658